LANDSLIDES FROM MASSIVE ROCK SLOPE FAILURE AND ASSOCIATED PHENOMENA

S.G. EVANS[1]
Department of Earth Sciences
University of Waterloo, 200 University Avenue West,
Waterloo, Ontario, Canada, N2L 3G1
G. SCARASCIA MUGNOZZA
Department of Earth Sciences
University of Rome "La Sapienza", P. le A. Moro, 5, 00185 Roma, Italy
A.L. STROM
Institute of the Geospheres Dynamics, Russian Academy of Sciences, Leninskiy Avenue, 38-1, 119334, Moscow, Russia
R.L. HERMANNS
Geological Survey of Canada
101-605 Robson Street Vancouver, British Columbia, Canada V6B 5J3
A. ISCHUK
Institute of Earthquake Engineering and Seismology,
Academy of Sciences, Dushanbe, Tajikistan
S. VINNICHENKO
The Focus Organisation, Dushanbe, Tajikistan

Abstract

Landslides from massive rock slope failure (MRSF) are a major geological hazard in many parts of the world. Hazard assessment is made difficult by a variety of complex initial failure processes and unpredictable post-failure behaviour, which includes transformation of movement mechanism, substantial changes in volume, and changes in the characteristics of the moving mass. Initial failure mechanisms are strongly influenced by geology and topography. Massive rock slope failure includes rockslides, rock avalanches, catastrophic spreads and rockfalls. Catastrophic debris flows can also be triggered by massive rock slope failure. Volcanoes are particularly prone to massive rock slope failure and can experience very large scale sector collapse or much smaller partial collapse. Both these types of failures may be transformed into lahars which can travel over 100 km from their source. MRSF deposits give insight into fragmentation and emplacement processes. Slow mountain slope deformation presents problems in interpretation of origin and movement mechanism. The identification of thresholds for the catastrophic failure of a slow moving rock slope is a key question in hazard assessment. Advances have been made in the analysis and modeling of initial failure and post-failure behaviour. However, these studies have been retrodictive in nature and their true predictive potential for hazard assessment remains uncertain yet promising.

[1] *E-mail of corresponding author;* sgevans@uwaterloo.ca

S.G. Evans et al. (eds.), Landslides from Massive Rock Slope Failure, 3–52.

Secondary processes associated with MRSF are an important component of hazard. These processes, which can be instantaneous or delayed, include the formation and failure of landslide dams and the generation of landslide tsunamis. Both these processes extend potential damage beyond the limits of landslide debris. The occurrence of MRSF forms orderly magnitude and frequency relations which can be characterized by robust power law relationships. MRSF is increasingly recognized as being an important process in landscape evolution which provides an essential context for enhanced hazard assessment.

1. Introduction

1.1. MASSIVE ROCK SLOPE FAILURE

Landslides from massive rock slope failure (MRSF) are a major geological hazard in many parts of the world [e.g., 2, 29, 85, 96, 110, 267, 282, 325, 326, 342, 303] and have been responsible for some of the most destructive natural disasters of recent history [54; Evans, this volume]. They involve the initial rock failure mass but may also incorporate a variety of earth materials entrained in its path [2, 3, 148], and exhibit a range of landslide volumes covering at least five orders of magnitude between 10^5 and 10^{10} m^3.

We use the descriptor "massive" in this context not only to describe large or unusually large massive rock slope failure but also with reference to the resultant geomorphic and socio-economic impact. This hybrid definition of massive therefore encompasses a wide range of primary landslide and secondary phenomena.

Landslides resulting from massive rock slope failure are frequently multiple phase landslides in which, for example, a disintegrating rock mass involved in an initial rockslide and subsequent rock avalanche becomes transformed into a massive, rapid debris flow which travels well beyond expected limits [e.g., 45, 134, 275, 276]. It is thus difficult to classify landslides from MRSF using recently proposed landslide classification schemes [e.g. 78, 72], although the scheme proposed recently by Hungr at al. [163] appears to be useful for the classification of flow-type landslides resulting from MRSF.

Secondary processes associated with massive rock slope failure are an important aspect of the phenomena. They include landslide-generated waves and displaced water effects [e.g., 124; Blikra, this volume; Ghirotti this volume] and those associated with landslide dams [e.g., 204, 350]. Catastrophic secondary effects may be instantaneous or delayed and extend the impact of a landslide beyond the boundaries of the primary landslide debris.

1.2 THE COMPLEXITY OF THE MASSIVE ROCK SLOPE FAILURE PHENOMENON

The complexity of the massive rock slope failure phenomenon is best exemplified by a field example. Figure 1 shows a typical field situation encountered in the mountainous regions of the world. It shows rock avalanche deposits which originated in a dip-slope of folded 33-41° east dipping Cretaceous conglomerates in the Tonco valley, NW-

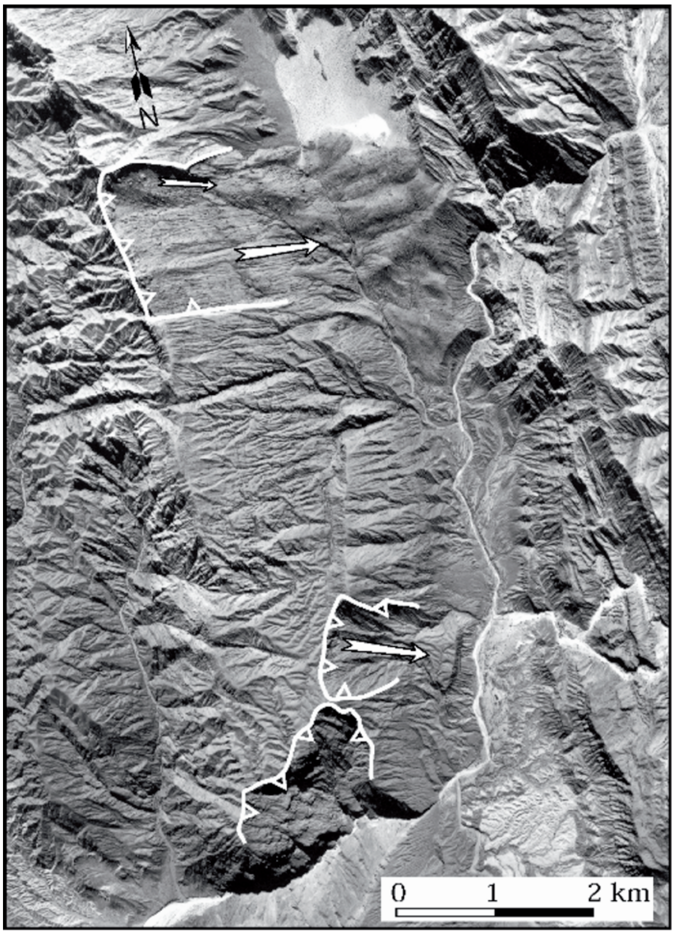

Figure 1. Aerial photograph of massive rock slope failure in the Tonco valley, northwest Argentina (see text for discussion).

Argentina [see Hermanns et al. this volume]. Different ages of rock avalanches can be inferred from boulder size, landslide- and breakaway-scarp morphology. In the north, at least two rock avalanche deposits overlie each other. The older larger rock avalanche, which originated from the collapse of a block 1.4 km wide, 1 km long and 50 m thick, dammed the Tonco valley. While the main river (flowing from NE to SW, entering from the right of the photograph) could erode through this natural dam, the tributary stream (from the N, entering from the top of the photograph) could not , thus causing the filling up of the small landslide-dammed basin by sediments. This deposit is overlain by a smaller rock-avalanche deposit which originated from the collapse of the northern break-away scarp of the older rock-avalanche and can be distinguished from the older deposits by larger and more abundant mega-blocks on its surface.

In the south the remains of an older rock-avalanche deposit exists. At this site the break-away scarp is much more deeply eroded and no mega-blocks are preserved at the surface of the strongly eroded deposit. A possible eroded break-away scarp suggests that at least one further landslide occurred in the wall of the deeply incised canyon which represents the outlet of the Tonco valley. Along this canyon, in some segments not more than ~1 m wide, possible landslide deposits would have been rapidly removed by erosion and thus whether a rock slope failure took place at this location is uncertain.

Figure 1 illustrates several issues related to MRSF; the role of structural control (dip slope) on initial failure and rock avalanche recurrence, deposit morphology, the interpretation of possible sources of rock slope failure, landslide damming with related fill-up of basins and lake sediments, and the problems of interpreting the sequence of rock slope failure events. The example and the dating of this sequence of failures are described in more detail by Hermanns et al (this volume).

1.3. OBJECTIVES

Our objectives in this introductory chapter are to review the range of landslides associated with massive rock slope failure with an emphasis on recent research, new events, and new data on already well known rockslides, rock avalanches and landslides involving volcanoes. Where possible, examples will be drawn from the countries of the former Soviet Union, particularly Russia, Kyrgyzstan and Tajikistan in an attempt to fill an information gap on important rock slope failures from this region. We also briefly touch on recent thematic developments in the analysis and modeling of initial and post-failure behaviour of massive rock slope failure. Finally, we highlight recent research on spatial/ temporal patterns of occurrence which have led to new insights into the role of MRSF in landscape evolution.

2. Initial Rock Slope Failure (Excluding the Failure of Volcano Slopes)

The mode of initial failure in bedrock slopes is strongly controlled by slope geometry and geologic structure, including rock mass fabric and lithology contrasts in the source slope [e.g. 50, 65, 69, 123, 127, 265, 299].

In sedimentary rocks and bedded volcaniclastic sequences, sliding frequently takes place along persistent planar discontinuities such as bedding planes (Figure 2), faults, joint surfaces, or lithologic contacts. In dip slopes, sliding takes place on bedding planes [e.g., 31, 48, 66, 84, 102, 115, 136, 140, 156, 259].

Sliding is frequently facilitated by the presence of bedding plane shears resulting from tectonic processes [e.g., 98, 333], gouge zones, or weak primary interlayers such as tuffaceous zones [104], shale, marl, or clay interbeds [138]. Dip-slope sliding may be facilitated by buckling [e.g., 312, 333] or by shear across bedding [104]. Initial failure in steep underdip slopes, and reverse slopes in bedded rock sequences is more complex and may involve buckling [154], toppling [68, 230] or break-out across bedding [100]. The dip of key discontinuities may vary in a given dip slope and the sliding surface may thus be concave [e.g., 100] or convex [e.g. 118, 140, 333]. Buckling and break-out are important failure mechanisms in these cases [Scarascia-Mugnozza et al., this volume].

Planar or gently curved discontinuities are also important in determining failure mode in plutonic [e.g., 140, 344] and strongly foliated metamorphic rocks [94, 95, 124, 140, 332]. In structurally complex rocks, failure is controlled by impersistent but closely spaced discontinuities independent of lithology [e.g., 217, 248] and may be complex in detail consisting of single or multiple wedges combined with local toppling.

Figure 2. The breakaway scarp and sliding surface of the Avalanche Lake rock avalanche, Mackenzie Mountains, North West Territories, Canada [102]. The sliding surface consists of a bedding plane in Paleozoic carbonates that form a dip slope, evident in background.

In very steep slopes, in steep mountain peaks or coastal cliffs for example, high angle detachment may occur along surfaces consisting of vertical to high angle tension cracks below which tension failure may follow suitably oriented discontinuities [e.g., joints] and at the base, failure occurs by shear through an intact wedge of material [e.g., 19, 80, 164]. In coastal cliffs the development of an erosional notch at the base of the cliff can reduce or eliminate the resistance of the passive wedge [19, 211] which may also result in a toppling failure [Stead, this volume].

Initial failure may be preceded by observable slope deformation. This is manifested in developing and widening tension cracks, increased rockfall activity and increasing disaggregation of the initial failure mass on the slope [e.g. 124, 169, 305, 306]. The description by Leopold Muller [228] of the development of the perimetral crack in the Vaiont slope as early as 1960 remains a chilling testimony to the need for correct interpretation of such movements [see Petley and Petley, this volume]. Time-to-failure calculations may be made on the rate of movement of survey stations on the moving slope, as recently reviewed by Crosta and Agliardi [64]. The complexity of prefailure creep movements is described by Varga (this volume).

Initial rock slope failure may occur without warning, however, as a result of a sudden earthquake trigger [e.g., 135, 217, 249], conventional and/or nuclear explosions [e.g., 5; Adushkin this volume] or as a result of sudden heavy rains [124, 275]. Some of the largest and most destructive massive rock slope failures in recent history have been triggered by seismic forces [181, 183, 264], such as the Tsao-Ling, Chi-fen-erh-shan, and Usoi rockslides, and the Khait and Mount Cook rock avalanches. Strong earthquakes may also simultaneously trigger a large number of massive rock slope failures over a large area as in the case of the M= 8.5 Great Alaska earthquake of 1964 [255], the M=7.0 1991 Racha earthquake in Georgia [24] and the 2002 M=7.9 Denali Fault earthquake in Alaska [83, 131].

3. Catastrophic Rockslides

A rockslide results from initial bedrock slope failure if distance of travel is limited, disintegration of the slide mass is incomplete, and if a significant amount of debris remains on the initial sliding surface [e.g., 32, 130, 247]. Catastrophic rockslides are characterised by high velocity despite the fact that the vertical displacement of the centre of gravity may be relatively small. High velocity requires some type of dramatic initial strength loss through such processes as brittleness of internal shears [165], or passive failure of intact rock in the toe region of the landslide [76, 296]. Although emplaced rapidly, rockslide debris frequently contains massive transported blocks of relatively undisturbed bedrock as at Kőfels, Flims, Usoi and Vaiont.

In the case of the Vaiont rockslide, catastrophic failure occurred on a sharply curved (concave) chair-like pre-existing sliding surface in Cretaceous limestones interbedded with clay layers on which sliding took place [138, 277, 278,279, 311, Ghirotti, this volume]. The Vaiont debris reached a peak velocity of 20-30 m/s in ca. 25 s of movement during which the centre of gravity was displaced a vertical distance of only 130 m. The brittleness implicit in this high velocity continues to be the subject of discussion [e.g., 165; Petley and Petley, this volume].

3.1. THE 1911 USOI ROCKSLIDE AND LANDSLIDE DAM, TAJIKISTAN

The world's largest known historical rockslide occurred in February 1911 in the Pamir Mountains of Tajikistan. The landslide was triggered by the M~7.4 Pamir Earthquake [117, 256, 271, 284, 351].

Figure 3. Sliding surface and breakaway scarp of the massive Rockslide Pass rockslide, Mackenzie Mountains, N.W.T., Canada. Sliding surface is a bedding plane in Paleozoic carbonates that dips at only 14 degrees.

The rockslide of ca. 2.2 B m^3 in volume, blocked the Murgab valley and formed 75 km long Lake Sarez [272]. It also blocked its left tributary – the Shaddau creek and formed a minor lake of the same name (Figures 4 and 5).

Sliding took place in Carboniferous and Triassic sedimentary rocks and during failure the centre of gravity was displaced in a vertical distance of about 500 m. The source zone of landslide is composed of two major rock units: 1) its upper part – Permo-Triassic dolomite, limestone, gypsum, and anhydrite) and 2) its lower part – Carboniferous Sarez Formation (sandstone, schist, and quartzite). The stratigraphic bedding mainly dips 30 to 45° towards NNW, with marked local variations due to internal folding and effects of small local faults. These formations are separated by the Usoi Thrust dipping 60 to 80° towards SE. In addition, there is a secondary (eastern) shear zone dipping 50° towards NW and the collapsed block was formed by the wedge bounded by these two fault planes (Figure 6).

The main part of the landslide body (Figures 5, 6, and 7) is composed of the debris of the Sarez Formation and its proximal part - of marble and shale with some subordinate gypsum, anhydrite and dolomite debris. Since the uppermost part of the source zone affected moraines of local hanging glaciers it is expected that some glacier ice may be buried in the proximal part of the landslide body. However, the internal composition of the Usoi Dam is not known. According to surface observations,

Figure 4. The Usoi rockslide shortly after it occurred. Scar is arrowed (white arrow at right). View is downstream. Lake Shaddau is to the left (S) and Lake Sarez is at the right (LS). Photograph was taken before the complete filling of Lake Sarez behind the rockslide dam (Plate I in Preobrajensky, 1920 [256]).

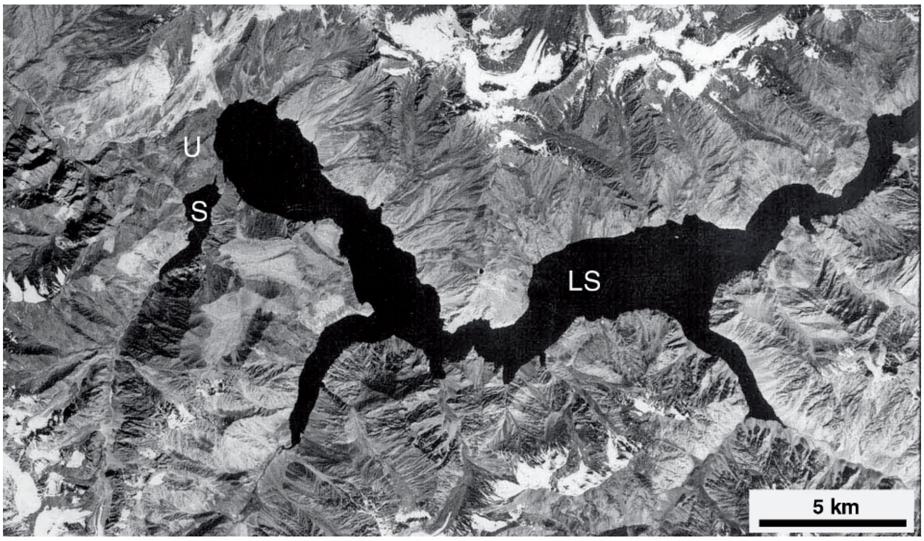

Figure 5. Satellite photograph of the Pamir Mountains, Tajikistan, showing the 1911 Usoi Landslide (U) which blocked the Murgab River to form Lake Sarez (LS) and Shaddau Lake (S).

significant variations in granulometry can be expected, with the grain-size composition of different parts of debris ranging from sandy-silty fines to blocks tens and hundreds of cubic meters in volume. Three main parts of the dam body can be identified;

1. The southern part is the highest part of the dam with a maximum height of about 250-270 m above the present-day lake level. Its surface is covered by angular blocks of Carboniferous rocks from 2 to 20 m and no fines are visible on the surface. Just along the southern border of the dam body one can see the moraine deposits composed of boulders and pebbles with fine loamy matrix. Similar deposits can be seen near the Shaddau Lake. Since they contain some granite boulders it is clear that the moraine material, at least that, resting at the Shaddau mouth, was scraped by the moving rockslide from the Murgab valley bottom.
2. The Central part of the dam body rises up to 100 m above lake level on the average and is bounded by an expessive escarpment facing to the downstream slope of the dam. It is clearly seen on the space images that this part of the dam was formed by a tremendous block of Carboniferous deposits (Figure 6) with preserved stratigraphy, though intensively fractured. At some places its surface is the "natural slope surface" displaced from its original position.
3. Northern part of the dam is the lowest one and is only 38-45 m above the lake level. It is covered by the large blocks of sandstone and shirts with the diameters from 2 to 20 m without fines. It can be expected that the frontal and proximal blocky zones represent outer parts of the huge block which central part remained more intact though fractured.

The dams surface abut to the foot of the scar and right flank of the Murgab River is covered by the deposits of the subsequent rockfalls, debris flows and mudflows with limestone, marble, gypsum and fine material of moraine deposits that came from the glacier valleys above the scar. This secondary deposits extents along the right part of the downstream slope of the dam up to the head of the erosional canyon. The latter is forming by the water filtrating through the dam. Previously it was also eroded by the mudflows from the glacier valleys above the scar that went in this direction. But since 1934-35, when rockfall from the scar wall diverged mudflows towards the lake, canyon is eroded only by springs.

Several north-south trending arcuate escarpments are clearly visible in the central and southern parts of the dam (Figure 6). The first step from the upstream looks like the ridge with very steep slope (60-70 degrees). Investigations performed in the 1960s and 1970s show that infiltration in the dam takes place mainly in the narrow zone 100-130 meters below water level and that the dam' body below is impervious. The level of the lake is characterised by slow but gradually increase with annual variation about ± 6 m. Filtrating water first appeared as the lake level reached about 3100 masl (about 160 m below the present day level) and at present forms 57 powerful springs in the erosional canyon 140-150 m below the lake level (Figure 6). The discharge from all springs is 45-75 m^3/s (season variation) and depends on the lake level. No evidence of internal erosion has been found to date. Filtration takes place through the opened fractures in the uppermost blocky unit.

No vertical deformations have been directly measured on the landslide's surface since 1947. However, according to measurements performed in 1915 and in 1967, differences in elevations have reached 1-20 meters.

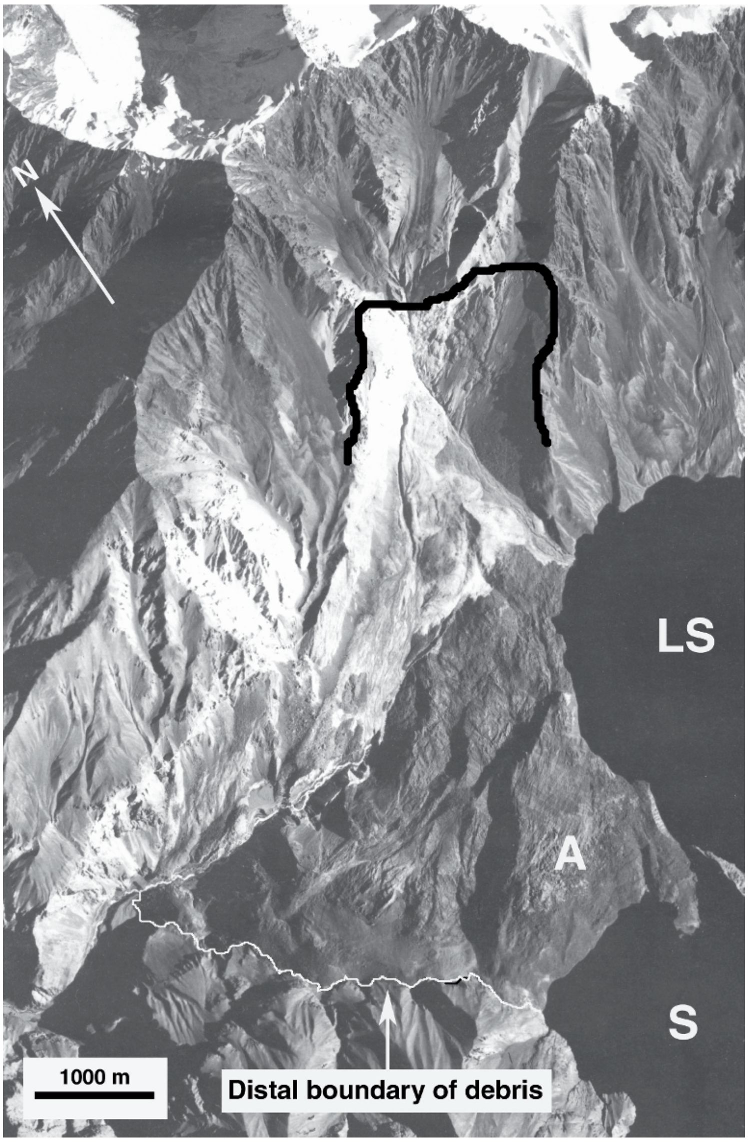

Figure 6. Satellite photograph of Usoi rockslide dam. Approximate distal boundary of debris is indicated. A = Massive intact slab mentioned in text; LS = Lake Sarez; S = Shaddau Lake

Analysis of the Usoi Landslide body and source zone allow a reconstruction of the mechanism of the earthquake-triggered slope failure. It is hypothesised that the huge wedge of the rocks slid down rapidly as a single block. When it struck the valley bottom and the opposite slope it expanded along the valley axis, mainly in a downstream direction, which led to the formation of the above mentioned arcuate escarpments, downthrown downvalley. Lack of seepage through the lower part of the blockage can be explained as a result of the intensive comminution of the debris that compose the internal part of this natural dam forming a substantial impermeable core [239, 300, 301] as observed at the numerous dissected rockslide dams elsewhere in Central Asia [Abdrakhmatov & Strom, this volume, Hewitt, this Volume].

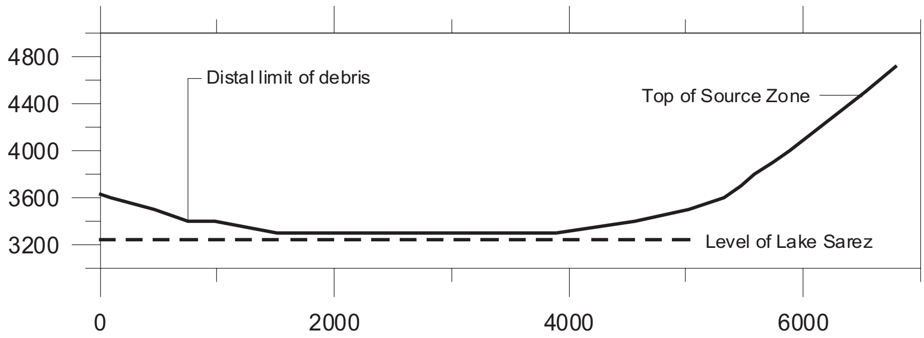

Figure 7. Profile of Usoi rockslide. Level of Lake Sarez (~ 3255 m.a.s.l.) is indicated. Profile suggests a fahrboschung of ~ 12 degrees.

3.2. DISTAL FLOWS AND ROCKSLIDES

Importantly, the debris of some rockslides exhibits partial mobility in which some of the debris disaggregates completely and is transformed into a fast moving debris flow or even a secondary rock avalanche, thus extending the distal reach of the movement [e.g. 98, 188, 231, 302]. An example is illustrated in Figure 8. The mechanism of distal flows is thought to involve undrained loading of valley floor sediments (see Section 7 below).

4. Catastrophic Spreads

Other styles of catastrophic bedrock slope instability develop in situations where a thickness of hard resistant caprock overlies weaker softer ductile rocks, such as tuffs, shales, or flysch sediments. This style of instability may involve toppling [89] and/or spreading of the subjacent weak layer and has catastrophic potential. Such movements are common in layered volcanic successions [90] where the caprock is lava, and in the thrust and nappe belts of the Alps [e.g., 199] and the Rocky Mountains of North America [174] where the cap rock is frequently overthrust Proterozoic or Paleozoic limestone and the subjacent material is Cretaceous shale.

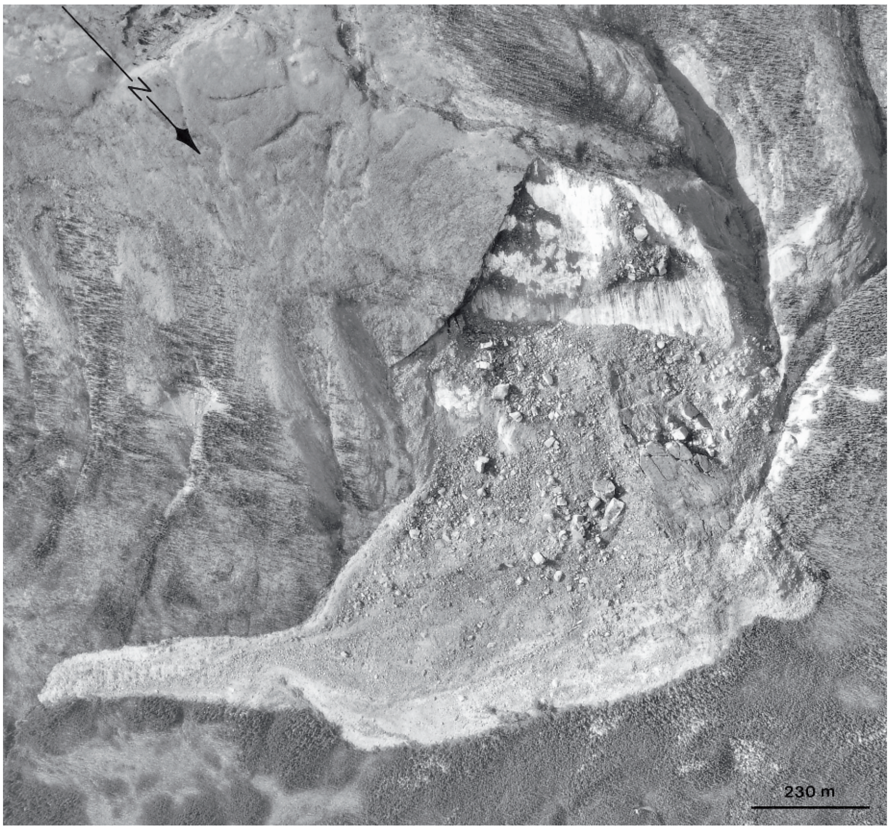

Figure 8. Vertical aerial photograph of North Nahanni rockslide, N.W.T. Canada (98). The landslide was triggered by the October 1985 North Nahanni earthquake. Note tongue-shaped distal flow that ran out from main debris deposit (98).

Spreads can be catastrophic. On June 24, 1765, a catastrophic spread destroyed the village of Roccamontepiano in central Italy resulting in more than 500 deaths [11, 62]. At the site, 30 – 40 m of resistant Pleistocene travertine forms a rigid cap rock which overlies weaker subjacent Upper Pliocene marine clays. Failure occurred as deformation in the subjacent clay led to tensile failure in the travertine cap which then was free to load a soft clay foundation leading to a catastrophic collapse of the sequence [75]. The catastrophic collapse took place only hours after the first signs of instability in the travertine cap.

5. Rockfalls

Rockfall involves the fall of a rock mass following initial detachment from a very steep rock slope, its disintegration and subsequent movement which may involve bouncing, rolling, or sliding generally down the steep source rock slope. Massive rock falls frequently transform into highly mobile debris flows or rock avalanches as in the case of the 1970 Huascaran, the 1959 Pandemonium Creek, and several recent events in the European and New Zealand Alps [14, 99, 217, 249].

Rockfalls retain their identity as a landslide type when the initial failure volume is less than the threshold volume where mass flow does not result. This process has been termed fragmental rock fall [97]. The threshold volume for this transition varies with the source material. In hard non-porous rocks it is ca. 1 M m^3 and in soft porous rocks it is about 500,000 m^3. Although rockfalls, thus defined, are much smaller than rock avalanches and rock slides they are more frequent and may be highly destructive over a limited area.

Rockfalls can be a major hazard in mountain communities [8, 33, 97]. At Lecco, in the Italian Alps, for example, about 15,000 m^3 of dolomite broke away from a cliff above the town in 1969 [8]. The mass broke up and rockfall fragments smashed into homes below claiming 8 lives [8]. In the case of the Malpa rockfalls, which occurred in the Kumaun Himalaya of India in 1998, rockfalls dammed a steep watershed and the resulting dam-break debris flow overwhelmed Malpa Village claiming the lives of 221 people [243].

Rockfalls are also a common hazard in transportation corridors that traverse rocky terrain [e.g., 27, 161].

Rockfalls may attain high velocities [8, 97]. In 1996, a remarkable rock fall occurred in Yosemite National Park [318, 346] in which a large block of granite (est. volume 27-62,000 m^3) detached from a cliff, slid down a 50º slope for about 185 m and then launched itself into the air. The rock then fell in free-fall before impacting on a talus slope 500 m below its launch point. The impact after the free fall was measured on seismographs within a 100 km radius and based on these records it is estimated that the rock impacted with a velocity of 146 m/s (525 km/hr) (318). The rockfall generated a wind blast which knocked down trees for a distance of 300 m.

Rockfalls are the most frequent landslide type triggered by earthquakes [181].

6. Rock Avalanches

6.1. GENERAL CHARACTERISTICS

Initial bedrock failure results in a rock avalanche when the rockmass disintegrates, leaving the source surface completely, and travels a downslope distance far from its origin (e.g., 103; Figure 9). The term was first used to describe the 1903 Frank Slide in the Alberta Rocky Mountains by R.G. McConnell and R. W. Brock [214] in 1904.

Figure 9. Perspective view to the southeast of the 1997 Mount Munday rock avalanche on Ice Valley Glacier, Waddington Range, southern Coast Mountains. This digital image was prepared from aerial photographs flown on August 20, 1997, and consists of a DEM with an orthophoto drape. Note flow lines in the debris. Elevation of the top of the source area is 3000 m.a.s.l. and the lower tip of the debris is at 2100 m.a.s.l. The length of the rock avalanche path is 4.7 km [95].

Rock avalanches are extremely rapid movements. At the 1970 Huascaran event statements of eye witnesses suggested a mean velocity for the movement of 75 m/s (270 km/hr) with peak velocities perhaps as high as 277 m/s (997 km/hr) being indicated by the analysis of the ballistic trajectory of huge granodiorite blocks [249]. As recently reviewed by Wieczoreck et al. [346] some rock avalanches generate destructive winds. The 1984 Mount Cayley rock avalanche traveled so rapidly that it generated winds that not only felled mature trees but drove spear-shaped wood fragments into solid tree trunks along its margins (Figure 17 in [71]). Wind velocities in excess of 30 m/s (108 km/hr) are required to inflict this type of damage on mature pine trees [71].

During the course of a rock avalanche the debris may exhibit dramatic mobility effects in one or more of the following ways;

1. the surface of the moving debris shows superelevation as it passes through bends in its path (Figure 9; e.g., 99, 134).
2. abrupt changes in the direction of travel; the debris may run at right angles (Figure 9; e.g., 84, 94, 95), or even turn a full 180° to the original movement direction [99].
3. the debris may run over significant obstacles in its path [132 ; Hewitt, this volume], or run-up a considerable distance on opposing valley sides [91]. At the prehistoric Avalanche Lake rock avalanche, for example, debris ran up the opposite slope to a height of 640 m above the pre-landslide valley floor (Figure 10) [91, 102]. Excessive run-up has also been observed at rock avalanches in the Karakoram Himalayas as described by Hewitt [148; this volume].

Rock avalanches with volumes above about 1 M m^3 generally show a decrease in fahrböschung with volume [e.g., 55, 74, 123, 153, 186, 198, 270; Legros, this volume]. Landslides resulting from rock slope failures below this threshold volume may also show similar mobility behaviour when mobility is enhanced by such mechanisms as impact collapse, undrained loading, or fluidisation [e.g., 3, 105, 168, 266].

Interesting quantitative data on the dynamics of rock avalanche motion has been recorded during the study of the artificial rock avalanches (with volumes up to 4 M m^3), triggered by underground nuclear explosions [5, 6, Adushkin this volume] on Nova Zemylaya.

6.2. 1949 KHAIT ROCK AVALANCHE, TAJIKISTAN

One of the most destructive rock avalanches in recent history occurred on July 10, 1949 in Tajikistan when a large rock avalanche (Figure 11) caused by the $M_s \sim 7.6$ Khait earthquake destroyed the town of Khait with the loss of as many as 24,000 inhabitants [200]. The initial rock slope failure that caused the Khait rock avalanche occurred on the northern slope of the Chohrak Mountain (el. ~ 3076 m) in the upper reaches of the Obi-Khaus-Dara River, a tributary of the Obi-Kabud river, which, in turn, flows into the Surkhob River. Initial failure involved about 80 Mm^3 of Paleozoic

Figure 10. Excessive run-up at Avalanche Lake rock avalanche, Mackenzie Mountains, N.W.T. The landslide moved from the right and ran up the steep slope of the wall running out on the surface of The Shelf, 640 m above the pre-landslide valley floor [84, 91, 102].

gneiss. The left margin of the source zone coincided with the fault plane of the large fault and the collapsing mass slid along this smooth plane. It is thought that this fault was ruptured during the earthquake and displaced up to 0.7-0.8 m.

The 1949 rock avalanche was not the first massive rock slope failure in this area. Just upstream from the 1949 failure, the Obi-Khaus-Dara River is blocked by an ancient rockslide, several Mm^3 in volume, that dams a small lake (Figure 11). According to lichenometric dating, this failure occurred during the period from 1740 to 1880 AD [233].

One of the characteristics of the Khait area is the wide distribution of loamy loess deposits on the mountain slopes and river terraces. According to eyewitness reports, the earthquake was preceded by several days of rain (Leonov, personal communication) and the loess mantle appeared to be significantly saturated. Intensive seismic shaking led to widespread sliding of saturated loess downslope. As a result, the initial rockslide entrained a large amount of saturated loess, also mixed with water from the Obi-Khaus-Dara River, and finally its volume increased to about 400 Mm^3, approximately 5 times the original failure volume.

All this mass rapidly moved downstream in the Obi-Khaus-Dara River and entered the Obi-Kabud valley. It is estimated that the velocity was in excess of 30 m/s; a powerful air blast pushed ahead of the landslide which destroyed buildings, uprooted trees and threw them for hundreds of metres [292, 293, 294]. The debris spread over the valley floor forming a fan-shaped apron (Figure 11) from 12 to 75 m in thickness

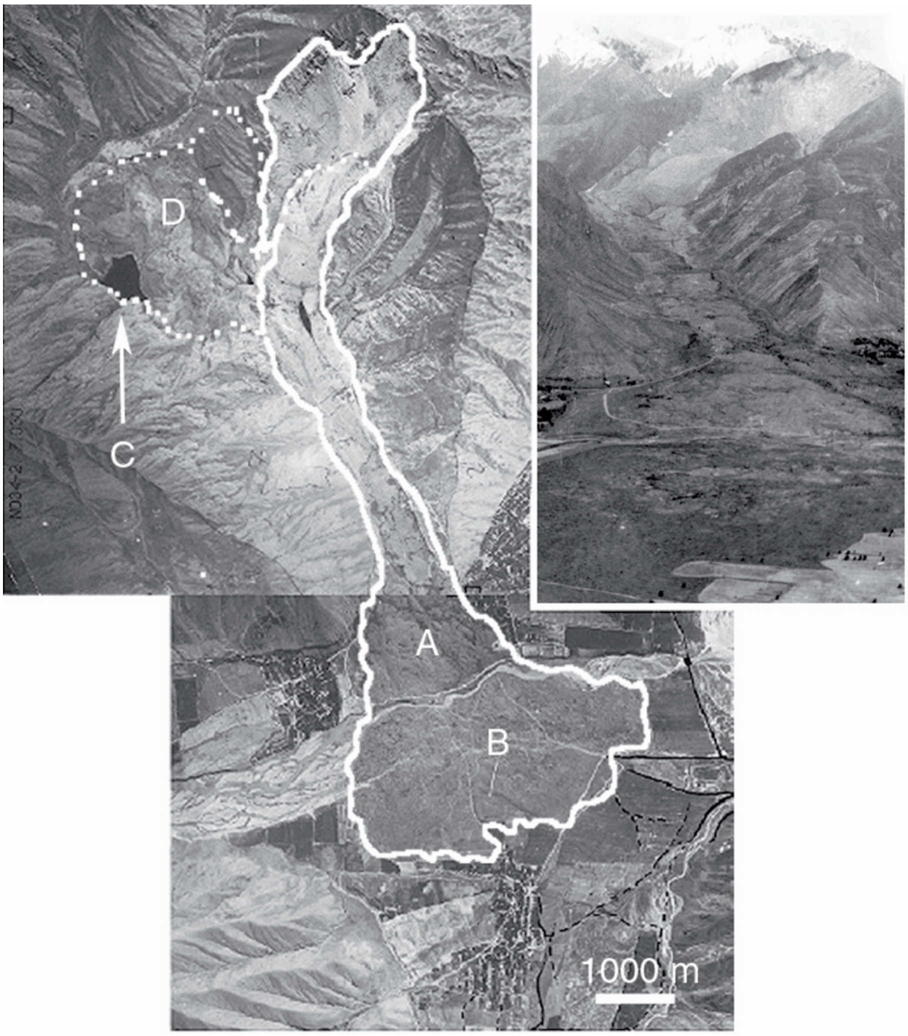

Figure 11. Aerial photograph mosaic of Khait rock avalanche, Tajikistan, which was triggered by 1949 Khait earthquake. The landslide source and path is outlined approximately. Town of Khait destroyed at A and village of Khisarak destroyed at B. As many as 24,000 people may have perished in these settlements. D is a prehistoric landslide dated by lichenometry to the 18th Century and C is a lake dammed by the landslide. Inset: aerial view of the Khait landslide toward the source area.

with numerous mounds (molards) formed by water spouting ("ground fountains") in the consolidating debris [294].

The debris buried the town of Khait and the neighbouring small village of Khisarak (Figures 11 and 12). As many as 24,000 people may have been killed in these settlements. The total runout of the Khait rock avalanche was about 11 km over a vertical distance of about 1500 m (H/L = 0.14; fahrboschung ~ 8 degrees); the final 5700 m of travel was over an average slope of about 3 degrees.

Figure 12. Aerial view of the Khait rock avalanche showing the source massive rock slope failure (top right) the middle path, where massive entrainment of loess took place, and part of the deposit which buried the town of Khait (bottom left) (USGS photograph).

7. Debris Flows Induced by Rockslope Failure

When debris from a rockslope failure impacts on channel or valley floor sediments a destructive debris flow may be mobilised that travels well beyond the margins of the initial landslide debris [3]. In the Swiss Alps, for example, the Bonaduz Gravels, which are about 50 m thick and extend up to 12 km upstream from the margins of the prehistoric Flims rockslide (est. vol. 9 B m^3) have been interpreted as resulting from a debris flow generated by the mobilisation of saturated valley fill by the rockslide [3, Poschinger et al., this volume]. Splash zones are sometimes formed around the debris by fluidised material displaced from beneath the debris [214] and compressional deformation structures may be formed in sediments beneath or adjacent to the debris sheet [3, 52, 254].

Similar effects may result from impacts of rockfall debris on saturated colluvium or talus forming the lower part of a valley side slope [Hungr, this volume]. At Fidaz, Switzerland a catastrophe occurred in 1939 when a rock mass fell (est. vol. 100,000 m^3) from the scarp of the prehistoric Flims rockslide and impacted a colluvial slope below. The rockfall entrained colluvial material increasing the volume of the debris to about

400,000 m^3. The rockfall/debris flow travelled rapidly downslope reaching a velocity of over 40 m/s. The debris reached a point 1.3 km from the source cliff and in its travel the landslide overwhelmed a children's sanitorium located below the cliffs causing 18 deaths [160, 232]. A similar event occurred in 1953 in Modalen, Norway, when a rockfall (est. volume 10,000 m^3) fell about 200 m onto a 30° talus slope [21, 192]. The impact triggered a flowslide in the talus (est. volume 100,000 m^3) which swept downslope and across level farmland, destroying two farm houses. The debris reached 200 m beyond the foot of the talus.

A well documented case occurred in Hawaii in 1981 [178]. In this case 500,000 m^3 of volcanic rock fell from a steep lava cliff, impacted on the canyon floor below and mobilized a large volume of material thus generating a rapidly moving debris flow that ran out a distance of 4.6 km. The volume of the debris flow was approximately 2.5 M m^3, about 5 times the volume of the initial rockfall [178].

More recently, a similar event occurred on Vancouver Island, Canada in 1999 (Figure 13). Detailed mapping has indicated that the volume of the initial rock failure was about 300,000 m^3. Impacting a saturated colluvial slope below, the rockfall entrained a further 350,000 m^3 of material. The debris flow, with a volume approaching 700,000 m^3, then turned sharply (Figure 13) and ran down the Nomash Valley for a further 1.75 km on an average slope of only 3 degrees.

Such responses of valley sediments and valley side deposits suggest that the impact loading of saturated materials can generate pore pressures which reduce the frictional resistance at the base of the moving debris; undrained loading generated by rapidly moving debris may thus be an important mechanism in explaining the anomalous mobility of certain rock avalanches and rockfall events [3, 266]. Further, the volume of entrained material from the landslide path may significantly enhance the volume involved in initial rock slope failure.

8. Landslides from Volcanoes

Volcanoes are highly unstable piles of ejecta and eruptive products and as such are the locus of frequent episodic landslide activity [7, 215, 219, 269, 327, 328], either in association with volcanic eruptions or during periods of qiuescence. Landslides from volcanoes include large-scale flank collapse and smaller scale landslides (volcanic debris avalanches) involving part of the edifice. Sometimes these massive rock slope failures are transformed into lahars (volcanic debris flows).

8.1. FLANK COLLAPSE

Massive catastrophic failure of the volcanic edifice itself has produced some of the largest sub-aerial landslides on earth; the Mount Shasta debris avalanche deposit, for example, is estimated to have a volume of 45 B m^3 [59] and the 18,520 y BP Nevado de Colima debris avalanche of Central Mexico is estimated to have a volume

Figure 13. The 1999 Nomash River rockfall/debris flow, Vancouver Island, Canada. A rock mass failure originated in the top right of the image and entrained a large volume of material from the valley side. The resultant debris flow traveled a further 1.75 km downstream on an average slope of only 3 degrees. Image consists of DEM draped with orthophoto.

in the range 22 - 33 B m^3 [298]. At Socompa volcano in northern Chile, a total of 53 B m^3 was displaced during the collapse of its northwestern flank at ca. 7,000 y BP [331] including a massive debris avalanche (est. vol. 26 B m^3) that flowed up to 40 km from the cone. Many volcanoes in the world have now been shown to have experienced major flank collapses during their existence [42, 112, 285, 286, 287, 289, 317, 320]. Multiple flank collapses have been documented at a number of volcanoes including Shiveluch volcano, Kamchatka, Russia where 8 collapses have been documented in the last 10,000 years [16].

Flank collapses may be triggered by magma emplacement, local tectonic displacements, oversteepening and/or overloading by the deposition of eruptive products, oversteepening and incision of the edifice by stream erosion, the generation of pore pressures generated as a result of magma intrusion or seismic shaking, and can also be induced by the degradation in the shear strength of materials within the edifice by low temperature hydrothermal alteration [260, 261, 286, 287, 202, 328, Reid and Brien, this volume]. Spreading of weak volcano foundations, first noted at some Indonesian volcanoes by van Bemmelen [321], may also lead to the deformation of a volcanic edifice and its subsequent catastrophic collapse [322, 323].

As with non-volcanic rock avalanches, the mobility of volcanic debris avalanches is directly related to volume. However, for a given volume, volcanic landslides resulting from flank collapse are more mobile, i.e., a lower fahrboschung, than their non-volcanic counterparts [198, 285, 330]. This may reflect amongst other factors, the common presence of large amounts of low strength hydrothermally-altered material rich in smectite in the landslide debris, the frequent inclusion of summit snow or ice caps in the failed mass which results in an increased water content, and a high degree of entrainment of material from the path of the landslide.

At least 11 flank collapses have taken place in the world since 1850 [286, 287, 288] including the massive eruption-related landslides at Mount Augustine, Alaska in 1883 (300 M m^3; [288]), Bandai-San, Japan, in 1888 (1.5 B m^3), Bezymianney, Kamchatka Peninsula, Russia, in 1956 (800 M m^3), Shiveluch, Kamchatka Peninsula, Russia in 1964 (1.5 km^3) and Mount St. Helens, Washington, U.S.A. (2.8 B m^3) in 1980. The 1888 Ritter Island lateral collapse, off the coast of New Guinea [177, 334] involved the mobilization of as much as 5 B m^3.

8.2. VOLCANIC ROCKDEBRIS AVALANCHES RESULTING FROM LIMITED EDIFICE FAILURE

Smaller scale landslides also occur on the slopes of volcanoes without involving the failure of a large part of the volcano's superstructure. Initial failure volumes are typically less than 100 M m^3 and commonly involve mechanically weak pyroclastic debris or hydrothermally altered rocks. Because of this, the "rock" mass involved in initial failure is easily fragmented and quickly becomes transformed into a rapidly moving rock/debris avalanche. Volcanic landslides of this type may be triggered by an eruption, small steam explosions, earthquake shaking, heavy rains, or glacier unloading [e.g., 60, 101, 125, 225, 339].

A typical example is the large prehistoric debris avalanche (est. volume 91 M m^3) on the slopes of Lastarria volcano in the Chilean Andes [229]. The initial slip surface parallels pyroclastic bedding in the volcano and the maximum travel distance of 6.7 km yields a fahrboschung of 8.5°. The pyroclastic debris is highly fragmented; near its distal limit, the debris ran up and over a small cone 125 m in height suggesting a minimum emplacement velocity of 50 m/s (180 km/hr).

In historic times, the Ontake debris avalanche/debris flow, triggered by the 1984 Nagano earthquake (M=6.8) in central Japan, is the best documented volcanic landslide of this type [e.g., 86, 225, 266, 329]. Initial sliding (est. vol. ~ 36 M m^3) involved failure of welded and non-welded scoriaceous pyroclastic rocks and lavas along a partially altered clayey pumice layer on the southeastern flank of Mount Ontake. The rockslide was quickly transformed into a rapid, highly-mobile debris flow which swept down the Denjo, Nigori, and Ohtaki rivers. Entrainment of deposits in these river valleys augmented the volume of the moving mass to an estimated 56 M m^3 [86]. The maximum travel distance was about 13 km over a vertical distance of 1600 m yielding a fahrboschung of 7º. Mobility of the debris avalanche may have been enhanced by the undrained loading of torrent deposits in the Denjo valley [266]. The average velocity of the landslide, based on eyewitness accounts, was 22 m/s with a maximum velocity estimated from super-elevation in bends of 36 m/s.

Volcanic rock/debris avalanches are frequently transformed into debris flows that travel beyond the limit of the debris deposited by the primary event [e.g., 101, 276] either by an immediate direct transformation of part of the debris into a distal mass flow or by the breach of a landslide dam formed by the debris sometime after it is deposited.

Debris avalanches from volcanoes have caused significant disasters in recent times. Most recently, in October 1998, a rock avalanche (est. vol. ~ 200,000 m^3) from Casita Volcano, Nicaragua, triggered by the rains of Hurricane Mitch, initially travelled about 3.2 km, [184, 275, 276, 283]. A debris flow originated from the rock avalanche debris, transforming the rock avalanche deposit into a rapidly moving fluid mass, which overwhelmed the villages of El Porvenir and Rolando Rodriguez 3 km further downslope. The debris flow travelled further downstream up to a distance of about 18 km from the limit of the initial rock avalanche deposit partially destroying many other villages. The immediate and delayed consequences of the event resulted in the deaths of approximately 2,500 people.

8.3. LAHARS RESULTING FROM TRANSFORMATION OF EDIFICE COLLAPSE OR MORE LIMITED EDIFICE FAILURE

Lahars are commonly associated with eruptions and may be triggered by a variety of processes including the melting of snow or glacier ice by hot ejecta, the ejection, or breaching, of the waters of a crater or caldera lake, the transformation of glowing ash avalanches, pyroclastic surges, or the transformation of an eruption-triggered flank collapse – debris avalanche [e.g., 338].

Some prehistoric lahars are enormous. Mothes et al. [227] have described the Chillos Valley lahar (est vol. 3.8 B m^3) in Ecuador that originated on the northern slopes of Cotopaxi volcano and travelled 326 km to the Pacific at about 4500 y BP. The lahar was generated by an ash flow following a small sector collapse which melted part of the volcano's ice cap and was transformed rapidly into the lahar. Further examples include a massive lahar (est. volume 1.8 B m^3), dating from the late Pleistocene, which originated from the edifice collapse of Citlaltepetl (5675 m) an ice-capped stratovolcano (43) in the trans-Mexican volcanic belt.

In the Cascade Volcanic Belt of the Pacific Northwest of the United States, work by Vallance and Scott [319] built on the classical descriptions of Crandell and Waldron [61] and Crandell [58] of the equally enormous Osceola Mudflow (est. vol. 3.8 B m^3), a lahar that originated in a sector collapse from the summit of Mount Rainier volcano about 4800 y BP. The Osceola Mudflow is estimated to have had a velocity of 19 m/s (68 km/hr) at 40-50 km downstream from its source. The 1980 collapse of Mt St Helens generated a massive lahar (est. vol. $10^8 m^3$) in the North Fork of the Toutle River by the delayed transformation of the flank collapse rock avalanche [175]. Scott [274] notes that it was formed by the dewatering of the avalanche deposit and slumping and erosion of its surface after a delay of about 5 hours. Flow velocity ranged from 6-12 m/s. Significant volumes of ice and snow may be contained in the intitial failure volume on snow/ice clad volcanoes and their melting contributes to the downstream transformation of flank collapse avalanches into long run-out lahars that may travel more than 100 km in valleys draining the source volcano [207].

9. Morphology, Internal Structure and Sedimentology of Massive Rock Slope Failure Deposits

The characteristics of MRSF deposits (morphology, internal structure and sedimentology) are important from a number of perspectives. First, they are essential in the initial identification of MRSF deposits. The MRSF literature is replete with examples of MRSF deposits that were initially interpreted as glacial deposits [e.g., 145, 238, 253]. As noted by Watson and Wright [335] even the colossal Saidmarreh rock avalanche, in the Zagros Mountains of Iran, was initially mapped as being the result of Pleistocene glaciation. Erroneous interpretations such as this led to underestimation of the extent of the occurrence of MRSF in the mountainous areas of the world especially in the Alps and Himalayas, which has been corrected only relatively recently.

Second, they give important evidence on the processes of fragmentation, transport and final emplacement/consolidation [e.g., 70, McSaveney and Davies, this volume; Poschinger et al., this volume] as well as the mechanism of the interaction with the substrate that the debris travels over [e.g., 254]. Morphological features of the deposit surface give indications of flow patterns [e.g., 216], emplacement sequence [e.g., 102] and post-depositional movement associated with consolidation of the debris. Sedimentological studies of prehistoric MRSF deposits have also shed light on the precise sequence of initial failure and possible secondary processes, such as distal debris flows initiated by impact loading of valley sediments or by dam break. In some cases this has led to a reinterpretation of prehistoric events as in the case of the Pleistocene debris-avalanche deposit from Nevado de Colima volcano, Mexico, which is now thought to largely consist of a 10 B m^3 dam breakout flow [41].

Third, knowledge of massive rock slope failure deposits and their internal structure is a key requirement in assessing the present stability of deposits that form landslide dams, either with respect to slope stability, piping, and/or resistance to overtopping [e.g., 44, 341].

Fourth, MRSF deposits are important foundation materials. Many built dams are constructed on natural landslide dams [e.g., 136, 308] and their material properties are required for geotechnical foundation design. In addition, many settlements in mountainous regions are situated on MRSF deposits and knowledge of their geotechnical characteristics is important in assessing their seismic response, particularly with respect to site amplification, and thus is important in seismic zonation.

Lastly, as the number of pits excavated in MRSF deposits around the world testifies, they are important sources of borrow material and thus a knowledge of their gradation has important consequences for their potential exploitation as a mineral resource.

Although a number of studies have been carried out on dissected landslide deposits in the present landscape, an important contribution to the knowledge of MRSF deposits has been made by a study of them in the geological record [e.g., 1, , 20, 113, 226, 349] where they have been termed “megabreccias” [e.g., 35, 195, 201].

10. Mountain Slope Deformation, Non-Catastrophic Rockslides, Catastrophic Failure Thresholds, and Problems of Origin

Evidence of mountain slope deformation is widespread in the mountain regions of the world [e.g., 9, 25, 26, 49, 50, 51, 63, 133, 212, 307, 324]. Mountain slope deformation consists of slow, deep-seated movement of a large rock mass that commonly exhibits loosening and fracturing in the sub-surface and signs of displacement on the surface of the slope itself slope surface. The process is termed “gravitational spreading” by Varnes et al. [324] and "sagging” by Hutchinson [166] who regards it as an early phase in the development of deep-seated landsliding. This type of slope movement may involve movement along discrete shear surfaces and/or deep seated mass creep [166]. It is commonly manifested in topographic features such as cracks, fissures, trenches, antislope (counter) scarps at mid or upper slope locations, and, in some cases, slope bulging at lower slope locations [e.g., 25, 26]. These linear geomorphic features may be collectively termed “sackungen”, after the German word for sagging [e.g., 213]. Frequently, these surface features occur without well defined headscarps, lateral scarps, or lateral shear zones suggesting that slope movement is occurring without the formation of well defined shear surfaces in contrast to rockslides described earlier.

Mountain slope deformation features (or sackungen) present difficulties in landslide hazard assessment in that (a) the precise movement mechanism is difficult to establish and thus to analyse, (b) the potential for the development of catastrophic detachment is difficult to evaluate, (c) the relationship to tectonic processes may be complex [e.g., 348] and (d) the origin of the linears themselves may be problematical, i.e. whether they represent a tectonic fault formed by an earthquake or a response to mountain slope deformation, is not always clear [e.g., 212, 310]. This issue is complicated by the fact that many examples of deep seated slope deformation occur in close association with pre-existing faults which may themselves be active. The problem of origin is also of concern in seismic hazard assessments for major engineering facilities in many countries such as Norway, Japan, the Cordillera of western Canada and neighbouring areas of the United States [e.g., 309].

The precise mechanism of mountain slope deformation is difficult to establish even at sites that have been extensively studied [235]. In the case of the slope above B.C. Hydro's Wahleach Power Station, in the Fraser Valley of southwestern British Columbia [224] an extensive slope stability investigation was began in January 1989 when the steel lining of a conduit tunnel leading down to the generating station was ruptured by slope movement. A major subsurface investigation established that no discrete sliding surface pre-existed or developed as a result of the movements.

Some sagging slopes are transitional to slow-moving rockslides. At Dutchmans Ridge, 1.5 km upstream from the Mica Dam in the Columbia Mountains, Canada, for example, detailed investigations by B.C. Hydro have shown that movement has taken place in the lower portion of the slope [170, 218, 222, 223]. Shortly after reservoir filling, downslope movement of about 10 mm/year was detected. It has taken place on a tectonic fault that dips toward the valley at 29º and involves 115 M m^3 of fractured gneissic and schistose rock.

As Steidl and Riedmuller [297] recently illustrated, deep-seated gravitational slope deformation can quite complex in detail. In their study, involving a slope in metamorphic rocks in the Austrian Alps, translational sliding at the head of the slope movement was driving deep-seated toppling at its base.

Indeed, where the geological structure is favourable mountain slope deformation frequently involves some degree of toppling [e.g., 50, 120, 251, 263] and/or sliding movement of a slope that has been previously disturbed by toppling. At the Clapière site in the French Alps, a moving slope consisting of migmatitic gneiss suddenly accelerated beginning in 1977 to create a major public safety issue [22]. The movements appeared to involve the slow sliding of a previously toppled slope in which the originally-vertical foliation in the slope decreased in dip by toppling forward thus creating a sliding surface for later movement [106, 107].

A major problem in the interpretation of massive rock slope movements is the prediction of the future behaviour of the slope and the establishment of conditions that determine the transition to possible catastrophic failure once ongoing mountain slope deformation has been detected [e.g., 120, 345, Bhasin and Kaynia, In press]. For example, the 1987 Valtellina rock avalanche took place in a slope that had undergone significant non-catastrophic deformation in the post-glacial period [124]. The boundary between non-catastrophic ductile flexural toppling and catastrophic brittle block toppling has been examined by Nichol et al. [230].

Large-scale non-catastrophic rockslides are common in many mountainous areas of the world, particularly in metamorphic rocks [e.g., 87, 119, 155, 171]. Rates of movement may be in the range of 1-2mm/yr.

11. Analysis and Modeling of Initial Rock Slope

The quantitative analysis of rock mass discontinuities coupled with the analysis and modeling of initial rock slope failure was slow to develop in engineering geology. One of the earliest quantitative attempts to relate the kinematics of massive rock slope failure to geological structure was that of Fuganti [115]. A classic early paper in the use of limit equilibrium analysis in the collapse of a rock slope was by Hutchinson [164]. The development of stability analyses based on limiting equilibrium for rock slopes and the use of stereographic projection techniques for kinematic analysis is summarized in Hoek and Bray [149] and more recently by Norrish and Wyllie [234]. Examples of complex limit equilibrium analyses of rock slopes are the work of Voight et al. [330], who analysed the 1980 failure of Mt. St. Helens, Hendron and Patton [138] who analysed the Vaiont rockslide, and Kaiser and Martin [208] who analysed a rock slope at the Revelstoke damsite, in British Columbia.

In extending analytical methods beyond limit equilibrium, early attempts in the use of finite element analysis in the analysis of large-scale natural rock slope movements were made by Kalkani and Piteau [180] and Krahn and Morgenstern [194]. Kohlbeck et al. [191] used a finite element model to analyse stresses in an alpine valley. Examples of later work using finite element techniques to analyse natural rock slope movements includes work by Hutchinson [167].

With the development of the Distinct-Element Method [73, 172] and the advent of UDEC and FLAC sophisticated numerical analyses of rock slopes became possible. Early work such as Pritchard and Savigny [257, 258] demonstrated their use in the analysis of movements in open pit slopes and natural rock slopes. Although extensively used in the analysis of excavated slopes in mines [e.g., 296] and construction sites little has been published, until recently, on the application of numerical methods to natural rock slope movements. Recent examples include work by Kimber et al. [187] on Portland limestone cliffs, Benko and Stead [17] on the 1903 Frank Slide, Voight [327] on the failure of andesitic volcanoes and lava domes, and others [9, 230, Bhasin and Kaynia, In Press]. These works have demonstrated the power of such methods to analyse kinematic scenarios as well as to model the actual failure mechanisms of the case in question. Such analysis requires detailed geological models and the accurate laboratory characterisastion of the materials involved in the movement [209].

In this volume, the numerical analysis of initial failure of natural slopes is reported in chapters by Scarascia Mugnozza et al., Eberhardt, Stead and Coggan, Genevois et al., and Merrien-Soukatchoff and Gunzberger. The reader is referred to a recent detailed review of numerical modeling for rock mechanics and rock engineering by Jing [176].

12. Analysis and Modeling of Post-Failure Behaviour of Rock Slopes

Substantial success has been achieved in the development of analytical models that simulate the bouncing and rolling of rockfall and rock-release fragments, the run-out distance and the velocity profile of rockfall [e.g., 28, 13, 158, 190, 246]. Calibration against observations of actual rockfalls has allowed a more rigorous selection of model parameters which govern rockfall motion [e.g., 12, 46, 97].

Transport mecahnisms of long run-out rock avalanches have been the subject of considerable research over the last twenty five years [e.g., 39, 40, 74, 157, 295]. Numerous mechanisms have been proposed to account for long run-out. These include various types of bulk fluidisation of all or part of the debris sheet, the generation of low friction (air, melted rock or liquefied substrate, snow ice) at the base of the mobile debris sheet, and those that invoke changing mass/rheology. Attempts to model these processes have met with a degree of success and have ranged from simple slide-block frictional models to those involving complex rheology [e.g., 157, 159, 162, 173, 268, 295, Crosta, this volume].

Retroactive simulation, or hindcast analyses, of individual catastrophic events utilising these models, in which model parameters are adjusted by trial and error, has successfully replicated run out distances, elapsed emplacement time, mean and peak velocities, and even debris sheet width and thickness [e.g., 157, 162, 315, Hungr, this volume]. Sousa and Voight [295], however, illustrate the uncertainties involved in the use of simulation models in real predictions of future landslide behaviour for hazard assessment.

13. Nature of Secondary Processes Resulting from Massive Rock Slope Failure – Instantaneous and Delayed

13.1. LANDSLIDE GENERATED WAVES (LANDSLIDE TSUNAMIS) AND DISPLACED WATER EFFECTS

Extremely rapid bedrock landslides that enter the sea, rivers, natural lakes, or artificial reservoirs generate displacement waves (landslide tsunamis) that may have catastrophic effects beyond the limits of the debris of the initiating landslide.

Landslide-generated waves in the sea; One of the greatest landslide disasters of the last millennium occurred on May 21^{st} , 1792, and resulted from the flank collapse of Mayuyama, a dacitic dome in the Unzen volcanic complex, on Kyushu Island, Japan [236; 240, 287, 289]. The massive landslide (estimated volume 340 M m^3) entered the Ariake Sea generating a tsunami which swept across and around the narrow enclosed sea [10]. The tsunami reached a height of 22.5 m at Musumi in Kumamoto Prefecture [316].

Other major tsunamigenic landslides from volcanoes in the Pacific occurred [196, 289] at Komagatatake, Japan (in the year 1640 – over 700 deaths in coastal villages), Oshima-Oshima, Japan (in the year 1741- 1475 deaths), Augustine, Alaska (in 1883), Ritter Island, New Guinea (in 1888 [177, 334], Harimkotan, Kurile Islands (in 1933) and Iliwerung, Java (in 1979 – 500 deaths).

Destructive displacement waves are also generated by landslides entering the waters of narrow fjords or confined bays [291]. Several examples have been documented in Norway [179; Blikra et al., this volume] Perhaps the most incredible landslide-generated wave is that which occurred in Lituya Bay in 1958 as a result of an earthquake triggered rock avalanche [114, 206, 220]. The rock avalanche (estimated volume 30 M m^3) impacted on the waters at the head of the bay and generated a wave run-up of 524 m, the highest recorded in history. The 1958 wave destroyed forest over an area of 10 km^2 and was the fourth or fifth to have occurred in Lituya Bay in the last two centuries [220].

More recently, in November 2000, a rockslide into the sea on the west coast of Greenland generated a tsunami that swept along the shores of the narrow Vaigat Strait in the vicinity of Paatuut. No lives were lost but 10 boats were destroyed and the abandoned coal-mining village of Qullissat was severely damaged [244].

Landslide-generated waves and displaced water effects in lakes: Water displaced by landslides entering lakes may have two effects, i.e., along the shoreline of the lake or downstream of the lake outlet. Huge waves may be generated by landslides entering confined lakes. On Vancouver Island, for example, a rock avalanche debris generated a wave in Landslide Lake that ran up a vertical distance of 51 m on the opposite shore [92] snapping mature cedar trees like matchsticks. At Mt St Helens in 1980, a lobe of the rockslide-avalanche resulting from the sector collapse of the volcano, entered Spirit Lake and generated a displacement wave that ran up 260 m above original lake level [330].

Landslide-generated waves may cause considerable destruction along the lakeshore, particularly at locations directly opposite the landslide source. A number of historical examples in Norway are described by Jorstad [179] including devastating events at Loen Lake in 1905 and 1936. In January 1905, a rockfall (est. vol. 50,000 m^3)

occurred on the west side of the lake; it incorporated till and talus from the valley side at the base of the rock slope forming a rapidly moving mass of about 300,000 m^3 which entered the lake below. The resulting waves caused widespread destruction along the lakeshore resulting in 61 deaths; the maximum vertical wave height was estimated to be 40.5 m. In 1936 another rockslide occurred on the west side of Lake Loen, just to the north of the 1905 scar. On this occasion, 1 M m^3 of debris entered the lake causing a huge wave which killed a further 73 people; the wave travelled at approximately 25 – 30 m/s (90 – 108 km/hr) along the lake shore [179]. The highest wave runups were directly opposite the landslide source area where a maximum of 74.2 m was recorded.

In March 1971, a major disaster occurred at Chungar in the Peruvian Andes. A wave, generated by a small rock avalanche (est. vol. 100,000 m^3), struck a mining camp located on the shore of a small lake and killed an estimated 400 people [250]. The wave washed up the opposite shore to a vertical height of 30 m and reduced bunkhouses constructed with concrete blocks to rubble [250].

A large landslide entering a small lake may also displace a large volume of lake water which subsequently travels downstream as a high velocity flood wave. In doing so material from the valley floor may be mobilised and entrained resulting in sediment concentrations approaching that of a debris flow [92, 121, 336]. A more complex case in which displaced lake waters augment the moving mass of a rapidly moving landslide occurred in Iceland [189] in 1965. A rock avalanche, consisting of rock and glacier ice (1 M m^3), fell onto a glacier. Part of the debris together with snow from the surface of the glacier entered a lake. Waters of the lake were displaced downstream in what could be termed a rockfall wave-outburst flood. The flood wave reached more than 25 km downstream. Similar events have been documented in Alaska by Wiles and Calkin, [347] and in New Zealand by McSaveney [217]. In the case of the 1987 Valtellina rock avalanche, the only fatalities from the landslide occurred when the rock avalanche displaced waters in a debris-dammed lake generating a catastrophic water-mud wave which overwhelmed part of the village of Aquilone claiming 27 lives [124].

Wavetrains generated by rockslope failure along the shorelines of landslide-dammed lakes may result in the overtopping of the landslide dam and its subsequent breaching [e.g., 337]. Further, wavetrains generated by rockfall or glacier avalanching are the major cause of the breaching of moraine dammed lakes [93] and other natural dams. Waves overtop the dam and initiate irreversible erosion leading to the catastrophic release of the water from the lake. These result in the generation of waterfloods, debris floods or debris flows downstream which themselves may be catastrophic as in the case of the 1941 Huaraz disaster in the Cordillera Blanca, Peruvian Andes [137, 205].

Landslide-generated waves and displaced water effects in artificial reservoirs; Artificial reservoirs form conditions which are especially vulnerable to catastrophic landslide-generated downstream water displacement because of the high volume of water in the reservoir and the substantial head difference at the dam. The 1963 Vaiont disaster in the Italian Alps is by far the worst recorded disaster caused by displacement waves in reservoirs. On October 9, 1963 a rockslide with a volume of approximately 270 M m^3 [138, Ghirotti, this volume] slid into the reservoir ponded behind the Vaiont Dam [185; 277], which at the time was the world's second highest dam (261.6 m high; crest elevation 725.5 m.a.s.l). The rockslide occurred very rapidly (20-30 m/s; [138])

and displaced a massive amount of water in the reservoir impounded behind the dam. The reservoir was two thirds full at the time and contained 115 M m^3 of water. A displacement wave ran up the opposite shore to el. 930 m., 230 m above the reservoir level and displaced about 25 M m^3 (ca. 22 % of the reservoir water) over the top of the Vaiont Dam [277]. As the wave overtopped the dam the maximum water depth was estimated to be 100 m. Seismograph data indicates that water was displaced from the reservoir over a period of 11 minutes with an average discharge of approximately 10^5 m^3/s (calculated from Selli and Trevisan, [277]).

As is now well known the concrete arch dam survived the overtopping and was left intact, but the displaced water ran down the Vaiont gorge and into the Piave river valley where it ran upstream and downstream, overwhelming several towns and villages including Longarone, Pirago, Villanova, Rivalta, and Fae. Approximately, 2000 inhabitants of the Piave valley lost their lives. The main loss of life was in Longarone (el. 473 m.a.s.l) which was overwhelmed 6 minutes after the frontal wave of the displaced water overtopped the Vaiont dam.

Landslide-generated waves may also damage facilities along the reservoir shoreline and damage the dam, possibly leading to a breach if waves overtop the structure. Many hydro-electric dams have been retrofitted with hardened crests to resist landslide-generated wave induced overtopping.

13.2. LANDSLIDE DAMS – UPSTREAM FLOODING AND DOWNSTREAM EFFECTS

Landslide dams form as a result of the blocking of drainage by landslide debris [4, 30, 57, 88, 136, 156, 193, 221, 340, 341, 350; Schuster, this volume]. Secondary effects resulting from landslide dams occur upstream as a result of water ponding up to the height of the dam (upstream flooding), or downstream due to the sudden release of the impounded water due to the catastrophic failure of the natural dam resulting in outburst floods [e.g., 280, 287, 350, 357]. Stable landslide dams may impound lakes that may become permanent features of the Holocene landscape [273] or form lakes that eventually disappear because of sediment infilling (147, 148, Schuster, this volume). Landslide dams may fail by overtopping, piping, or slope failure of the downstream face [e.g., 57, 88].

Outburst floods [56, 57, 143, 210] from landslide dams have been responsible for considerable death and destruction [Evans, this volume] in historical times. They are also of considerable geomorphic significance since they frequently reset fluvial systems downstream from the breach location and are typically orders of magnitude greater than the maximum probable "normal" hydrologic flood [e.g., 197]. The formation and failure of landslide dams during the travel of landslide debris may also augment the travel distance of landslide debris as in the case of the 1987 Parraguirre event, Chile [134].

Outburst floods from landslide dams have caused some notable disasters in China [203, 204] including what is probably the worst single-event landslide disaster of the millennium, the outburst flood on the Dadu River, Sichuan in 1786. [203]. The landslide, triggered by the Kangding-Louding earthquake, occurred at Momianshan, near Luding and was. It dammed the Dadu River for 10 days; when the dam was overtopped the dam failed and a great flood swept down the Dadu River as far as Yibin City, 1,400 km downstream. According to Li and Wang [203] the flood took as many as

100,000 lives along its path. One hundred and fourty seven years later, the Deixi landslide, triggered by the highly destructive Deixi earthquake, formed a 250 m high dam across the Minjiang River also in Sichuan Province, in 1933. The dam impounded the river for 45 days and failed rapidly after overtopping. Approximately 400 M m^3 of water was suddenly released in the flood which traveled a distance of 253 km downstream with an average velocity of 5.5 – 7.0 m/s; [204]. At least 2,423 people lost their lives.

Landslide dams have also been documented from many parts of the Himalayas [36, 108, 111, 144, 145, 146, 147, 148, 210, 332]. Three dramatic examples of landslide dam formation and failure are documented from the nineteenth century, *viz*. landslide dams on the Indus (1840 - 1841), which created the *First Great Indus Flood* of Mason [210], 1929, Hunza (1858), which created the *Second Great Indus Flood* of Mason [210], 1929, and the Gohna landslide (1893-94; [122, 150]). In the Indus case a large bedrock landslide, apparently triggered by an earthquake, blocked the mighty Indus, downstream from Gilgit, in what is now Pakistan, in January, 1841 [e.g., 15, 38, 53, 210, 241]. The landslide occurred on the left bank of the Indus at the western foot of the Nanga Parbat massif, in an area which is subject to an uplift of 7mm/yr and active neotectonics [37] and formed a lake which extended 60 km upstream, almost to Gilgit [el. ca. 1490 m.a.s.l.]. River elevation at the landslide location is 1178 m, and the full pool elevation of the impounded reservoir was about 1402 m.a.s.l [83]; the landslide lake filled in approximately 6 months and may have contained as much as 10 B m^3 of water, one of the largest bodies of water impounded by a natural dam documented on earth in the Holocene. In May 1841, warnings written on birch-bark were sent downstream urging inhabitants to flee from the rivers edge as it became obvious that the landslide dam would burst when it was overtopped [15, 139]. Early in June 1841, the blockage was breached. An enormous flood wave was released into the Indus as the contents of the lake apparently drained “off in a day” [79] and swept downstream *(The Great Indus Flood* of Mason, [210]). As summarised by Mason [210], the flood caused considerable destruction and great loss of life in the lower Indus valley, including soldiers of a Sikh army encamped at Attock who were overwhelmed some 320 km downstream from the landslide dam. Flooding also occurred in some Indus tributaries because of the hydraulic obstruction created by the flood waters. The rise in the Indus at Attock (>25 m) was the highest recorded and a conservative estimate of peak discharge is 2 M m^3/s [143]. The 1858 landslide dam on the Hunza River existed for 6 months before draining catastrophically. During this time at least 10-11 m of silt was deposited in the lake [242].

Typical deposits of outburst floods are terraces as described in the Indus valley and tributaries by Hewitt [144, 147]. A sequence of terraces defended by landslide barriers at different levels above the actual valley indicate therefore intermittent breaching of the barrier. Of high importance to dam stability is where the first outlet gorge forms. In the Karakoram 21 landslide dams of 96 cross-valley deposits have gorges within the bedrock and therefore at different position than the pre-landslide river course [144]. At such “epigenetic” gorges fluvial incision is controlled by the bedrock properties significantly different from the strongly shattered landslide deposits. Landslide dams with such type of outlets are less likely to fail catastrophically.

14. Magnitude and Frequency of Massive Rock Slope Failure and Its Role In Landscape Evolution

14.1. BACKGROUND TO LANDSLIDE MAGNITUDE AND FREQUENCY RELATIONS

Analysis and use of the magnitude and frequency (m/f) relations of landslides, is a comparatively recent development in massive rock slope failure hazard assessment (Evans, this volume). The approach is based to some extent on the well-known Gutenberg-Richter power-law relation [126] for earthquakes (1)

$$\log N(m) = aM^{-b} \tag{1}$$

where N(m) = cumulative frequency equal to or greater than M, M is earthquake magnitude, a and b are constants.

Because of its scale-invariance and universal characteristic (1) has formed the basis for seismic hazard assessment methodologies world-wide based on the analysis of earthquake occurrences recorded in historical earthquake catalogues supplemented by geological evidence for prehistoric earthquakes.

In its application to landslides, magnitude (m) has been taken to be some measure of landslide size based on area (A) or volume (V). Frequency (f) may be expressed in a simple cumulative (or rank-ordering), in a non-cumulative manner (see discussion in Guzzetti et al. [128]), or in terms of frequency density, i.e., the number of landslides in any given magnitude bin divided by the bin size [129]. Frequency may also be expressed directly as an annual frequency (cumulative number per year) if, as discussed below, the dataset is time constrained. The methodology is applied utilizing spatial datasets (landslide inventories) for a region representing landslide occurrence in various types of temporal records;

14.2. THE STRUCTURE OF LANDSLIDE MAGNITUDE/FREQUENCY RELATIONS

Early work by Fuji [116] analysed the m/f relationship for 650 rainfall-triggered events and found that the frequency of landslides is inversely related to their volume and can be defined by a power law similar to the Gutenburg-Richter relation in (1). Whitehouse and Griffiths [343] found a similar relationship for rock avalanches in New Zealand. Later work by Ohmori and Hirano [237] and Sugai et al. (304) further showed that landslide m/f relations are power law functions of magnitude.

However, it was the work of Hovius et al. [151] and Pelletier et al. [245] that initiated the current interest in landslide magnitude and frequency by deriving what can be described as the characteristic form of the magnitude/frequency relation. Hovius et al. [151] analysed multiple sets of air photos between 1948 and 1986 in the western Southern Alps of New Zealand. They found that m/f relations for the area of landslide scars (A_s) are scale invariant and had a robust power law m/f distribution over approximately two orders of area magnitude with a flattening of the curve at lower magnitudes. Pelletier et al. [245] analysed three data sets in which magnitude was expressed in terms of area (A); a data set of landslides in Japan, in which landslide area included the run-out zone, a data set of landslides in Bolivia, and a record of 11,111 landslides triggered by the 1994 Northridge earthquake over an area of 10,000 km^2. All three m/f plots showed a linear segment characterized by a power law and a flattening of the curve at small landslide magnitudes.

Thus the m/f log-log plots of Hovius et al. [151] and Pelletier [245] show two characteristics; first a liner segment at small to large magnitudes and second, a flattening of the curve at small magnitudes which has been termed "rollover". The linear portion of the m/f plot obeys a power law of general form in (2)

$$N\,(A) \sim A^{-b} \tag{2}$$

where A is landslide area, N(A) the number of events greater than V and b is a constant.

Subsequent studies on different types of landslides in different geological environments have found similar results and m/f plots of similar shape. Hungr et al. [161] analysed maintenance records for the volume and frequency of rockfall along transportation routes in British Columbia and found m/f relations characterised by a power law. Other studies of the m/f of rockfall and rock slope failure, using volume as magnitude, were carried out by Chau et al. [47] in Hong Kong, Guzzetti et al. [129] in Yosemite, and Singh and Vick [290] in British Columbia. All these studies found broadly similar m/f relations. In a comprehensive study, Dussauge-Pressier et al. [82] and Dussauge et al. [81] found that datasets of rockfalls from Yosemite and the Grenoble area as well as rockslides and rock avalanches from a global data set followed a m/f relation characterised by a power law in (2).

Thus the structure of landslide m/f relations is characterized by scale invariance (i.e., the power-law segment of the m/f plot is linear over several orders of landslide magnitude); similar shaped m/f plots are obtained for various measures of landslide magnitude consisting of area and volume, different landslide types, in different geological environments both in space and time, and with different triggers. The characteristic relation is obtained from the analysis of various types of temporal records. The characteristic m/f relation also applies to landslides from natural and artificial slopes in natural and human-modified terrain. The power law structure of the m/f relation makes it possible to predict the frequency of larger landslides (for which a record may not exist) based on the slope of the linear part of the m/f plot derived from the occurrence of smaller landslides, assuming that the record of smaller landslides is complete [Evans, this volume].

These apparently universal characteristics of landslide m/f relations result in their extreme usefulness for landslide hazard assessment; they form a type of hazard model which may be used in the quantification of landslide hazard which can serve as input into a quantitative risk calculation. Once a magnitude and frequency relation has been established for a region or a site, it may be used to estimate the probability of occurrence of a landslide of a certain magnitude providing the length of the record is known [e.g., 81, 161]. This gives a quantitative estimate of hazard which when combined with vulnerability data can give a quantitative estimate of landslide risk. The first application of landslide m/f relations to formal landslide hazard and risk assessment was by Hungr et al. [161]. In this study, m/f relations were derived for rockfalls from natural and artificial slopes in transportation corridors in southwestern British Columbia utilizing a set of very complete Type 3 records. These data gave the probability of rockfalls of a given size occurring in the narrow linear road and rail corridors. Combined with traffic density data for a segment of a corridor, the risk of a fatal accident due to rockfall impact was calculated [161]. It is also possible to use the m/f relations derived by Hungr et al. [161] to calculate the probability of such scenarios as total blockage of a given corridor by a large landslide involving massive rock slope failure.

14.3. ASSUMPTIONS AND LIMITATIONS IN THE MAGNITUDE/FREQUENCY APPROACH TO LANDSLIDE HAZARD ASSESSMENT

Despite the accumulating evidence of a characteristic, possibly universal landslide m/f signature there are some assumptions and limitations that should be kept in mind in the application of the methodology to landslide hazard assessment.

A major difficulty is the assumption of invariance in the occurrence of landslides in time, i.e., that the rate of occurrence implicit in the temporal records will persist at the same rates into the future, at least in terms of engineering time scales. Landslide occurrence reflects to some extent the frequency of landslide triggers (e.g., rainstorms and earthquakes). In this regard climate change may affect the frequency and intensity of rainfall triggers such that regional landslide events may be more frequent in the future. This could increase the frequency and thus the hazard of rainfall-triggered landslide events. At geological time scales, Cruden and Hu [67] have argued that the probability of occurrence of large rockslides in the Rocky Mountains of Canada is decaying with time as the number of rockslide sites conditioned by Pleistocene glaciation becomes exhausted by Holocene rockslide occurrence. This is in contrast to the implicit assumption of steady state landslide occurrence in landslide m/f relations.

Further limitations are associated with the quality of the landslide dataset. The accuracy of landslide magnitude measurement, whether it is expressed in terms of area or volume, is an important consideration. A related problem is that of record completeness. Erosion censoring of large magnitude landslides over long time periods removes them from long-time-period records [343]. In addition, the scale of spatial inventories determines the resolution of the record and the frequency count of smaller landslides.

Despite these assumptions and limitations, the analysis of landslide m/f relations, increasingly provides a key element in landslide hazard assessment and subsequent risk evaluation at regional and site scales.

14.4. MASSIVE ROCK SLOPE FAILURE AND QUATERNARY CLIMATE CHANGE

Ages of landslide dammed lakes and ages of landslide deposits have been compared to climatic periods in the Quaternary. For example, massive rock slope failures have been related in strongly glaciated regions with glacial retreat [e.g., 2, 67]. In Western Canada formation of recent rock avalanches has been shown to be a consequence of declining lateral support of valley walls by thinning of glaciers after the Little Ice Age [93, 95].

In a similar way, ages of landslide deposits in postglacial colluvium in western Norway coincides with the main deglaciation phase ~ 11 – 10 ka (23). Recent studies of rock avalanches in fjords of Norway show that older events (>10 ka) took place in the outer fjord areas while younger rock avalanches (3-6 ka) occurred in the inner parts of the fjords indicating the close link of slope collapse with deglaciation after the last Ice Age (Blikra, this volume). In semi-arid regions, run off along deeply incised valleys more likely influences slope stability. For example, along Rio Grande, New Mexico, large slumps damming the White Rock Canyon only occurred in the Late Pleistocene [77, 262]. No such mass movements are recorded from the Holocene along the Rio Grande, suggesting that slope destabilization was the consequence of downcutting of the river related to both glacial melt and enhanced pluvial activity in the late Pleistocene.

In NW-Argentina rock avalanche ages depend strongly on their geomorphic setting. While rock avalanches along mountain fronts [103] bordered by wide piedmont areas are relatively old and have recurrence intervals of several tens ka; those in narrow valleys are young, have recurrence intervals of a few ka and apparently cluster during periods characterized by more humid climate conditions in subtropical South America [141, 142, 313, 314; Hermanns et al, this volume] suggesting at these sites that stream power directly influence slope stability.

These examples highlight the impact of Quaternary climate change on rock slope failures. In the same way future climatic changes resulting in further deglaciation and/ or more humid conditions with a higher frequency of extreme meteorological events, are likely to influence the occurrence of massive rock slope failures in high mountain regions.

14.5. ROLE OF MASSIVE ROCK SLOPE FAILURE IN LANDSCAPE EVOLUTION

It has been recognized that, in tectonically active areas, bedrock landsliding is an important contributor to denudation and a major mechanism controlling mountain slope formation, valley incision and sediment flux [e.g., 34, 108, 109, 110, 151, Hovius and Stark, this volume].

Keefer [182], showed that erosion rates from earthquake-induced landslides vary significantly from region to region and that in some seismically active mountains such as western New Guinea, seismically-triggered landslides are the predominant agent of slope erosion. Hovius et al. [151] quantified denudation rates related to landsliding on the western slopes of the Southern Alps of New Zealand by analyzing aerial photographs spanning 60 years. Calculated erosion rates average 9 mm/yr and range from 5 to 12 mm/yr within individual catchments. Although these erosion rates are extremely high they coincide with areas of extreme rainfall and also high rock uplift, measured by fission track ages, thus a steady-state landscape can be envisioned in this mountain belt. In contrast, the Finisterre Mountains in Papua New Guinea are a young mountain belt in a pre-steady-state. Here, watersheds expand by large-scale landsliding controlled by ground-water seepage after their initiation as single gorges [152].

Landslide scars by themselves control further fluvial incision. These landslide controlled drainage patterns later only rarely are modified by further major landslides.

In the northwestern Himalaya, another mountain belt with high tectonic activity landslides from massive rock slope failure are widespread. Burbank et al. [34] could show that the Indus river surrounding mountains have average steep hillslope angles with a mean of 32 +/- 2°, which are independent of local erosion rates, suggesting control by a common threshold process where landsliding adjusts hillslopes efficiently between bedrock uplift and river incision.

Although these examples highlight the influence of landslides on hillslope formation, valley incision and sediment flux on regional scales, the volumetric impact of these processes by landslides are still poorly understood in many geologic and climatic settings.

15. Conclusions

Landslides from massive rock slope failure (MRSF) are a major geological hazard in many parts of the world and have been responsible for some of the world's major natural disasters. New mapping, and the reinterpretation of surficial materials previously mapped as glacial deposits, has led to a new understanding of the extent and frequency of massive rock slope failure in such regions as the Himalayas and the mountains of Central Asia in the countries of the former Soviet Union. Hazard assessment is made difficult by a variety of complex initial failure processes and unpredictable post-failure behaviour, which includes transformation of movement mechanism, substantial changes in volume by deposition and/or entrainment, and changes in the characteristics of the moving mass. Initial failure mechanisms are strongly influenced by geology and topography, and, because of this, the development of geological models is essential for the analysis of these mechanisms. Massive rock slope failure includes extremely rapid movements such as rockslides, rock avalanches, catastrophic spreads and rockfalls. However, catastrophic debris flows can also be triggered by massive rock slope failure and may present a significant hazard in themselves.

Volcanoes are particularly prone to massive rock slope failure and can experience very large-scale sector collapse, such as the 1980 flank collapse of Mt St Helens, or much smaller partial collapse, such as the 1984 earthquake-triggered failure at Mt. Ontake. Both these types of failures may be transformed into volcanic mudflows (lahars) which can travel over 100 km from their source.

Many cases of historical MRSF were preceded by precursory signs; movement monitoring data can be used to estimate time to failure. The study of MRSF deposits gives insight into fragmentation and emplacement processes. These studies are also important in the stability analysis of landslide dams. Slow mountain slope deformation presents problems in interpretation of both origin and movement mechanism. Geomorphic features related to slope sagging have been interpreted as tectonic faults. The problem of interpretation is made more difficult when mountain slope movement is related to the presence of tectonic faults. The identification of thresholds for the catastrophic failure of a slow moving rock slope is a key remaining question in landslide hazard assessment. Advances have been made in the analysis and modeling of initial failure and post-failure behaviour. However, these studies have been retrodictive in nature and their true predictive potential for hazard assessment remains uncertain yet promising.

Secondary processes associated with MRSF are an important component of hazard. These processes, which can be instantaneous or delayed, include the formation and failure of landslide dams and the generation of landslide tsunamis. Both these processes extend potential damage beyond the limits of landslide debris. The occurrence of MRSF in space and time forms orderly magnitude and frequency relations which can be characterized by robust power law relationships. Uncertainty about the temporal controls on MRSF occurrence condition the application of these relationships to hazard assessment. MRSF is increasingly recognized as being an important process in landscape evolution which provides an essential context for enhanced hazard assessment.

References

1. Abbott, P.L., Kerr, D.R., Borron, S.E., Washburn, J.L., and Rightmer, D.A. (2002) Neogene sturzstrom deposits, Split Mountain area, Anza-Borrego Desert State Park, California, in S.G. Evans and J.V. DeGraff (eds.), *Catastrophic landslides: effects, occurrence, and mechanisms*, Geol. Soc. Am. *Rev. Eng. Geol.*, v. XV, pp. 379-400.
2. Abele, G. (1974) Bergstürze in den Alpen, ihre Verbeitung, Morphologie und Folgeerscheinungen, *Wissensch. Alpenverein* **25**, 1-230.
3. Abele, G. (1997) Rockslide movement supported by the mobilization of groundwater-saturated valley floor sediments, *Zeits. für Geomorph*. **41**, 1-20.
4. Adams, J. (1981) Earthquake-dammed lakes in New Zealand, *Geology* **9**, 215-219.
5. Adushkin, V.V. (2000) Explosive initiation of creative processes in Nature, *Combustion, Explosion, and Shock Waves*, **36**, 695-703.
6. Adushkin, V.V. and Spungin, V.G. (1998) The influence (of) granular structure of rockfalls on their spreading along mountain slopes, in H-P. Rossmanith (ed.) *Proc. 3rd Int. Conf. on Mechanics of Jointed and Faulted Rock,* Vienna, Austria p. 541-546., A.A. Balkema, Rotterdam.
7. Adushkin, V.V., Zykov, Y.N., and Fedotov, S.A. (1995) Mechanism of volcanic slope failure; assessment of potential collapse and debris avalanches at Klyuchevskoi volcano, *Volc. Seism*. **16,** 667-684.
8. Agliardi, F. and Crosta, G.B. (2003) High resolution three-dimensional numerical modeling of rockfalls, *Int. Jo. of Rock Mech. and Mining Sci.* **40**, 455-471.
9. Agliardi, F., Crosta, G., and Zanchi, A. (2001) Structural constraints on deep-seated slope deformation kinematics, *Eng. Geol*. **59**, 83-102.
10. Aida, I. (1975) Numerical experiments of the tsunami associated with the collapse of Mt. Mayuyama in 1792, *Jo. Seismol. Soc. Jpn* **28,** 449-460 (in Japanese).
11. Almagià, R. (1910) La grande frana di Roccamontepiano (prov. Di Chieti) (24 giugno 1765), *Riv. Abruzz. di Sci. Lett. ed Arti*, **25,** 337-349.
12. Azzoni, A. and de Freitas, M.H. (1995) Experimentally gained parameters decisive for rock fall analysis, *Rock Mech Rock Eng*, **28**, 111-124
13. Azzoni, A., La Barbera, G., Zaninetti, A. (1995) Analysis and prediction of rock falls using a mathematical model, *Int. Jo. Rock Mech. Min. Sci.,* **32**, 709-724.
14. Barla, G., Dutto, F., and Mortara, G. (2000) Brenva Glacier rock avalanche of 18 January 1997 on the Mount Blanc Range, northwest Italy, *Landslide News* **13**, 2-5.
15. Becher, J. (1859) Letter addressed to R.H. Davies, Esquire, Secretary to the Government of the Punjab and its ependencies, *Jo. Asiatic Soc. of Bengal*, **28,** 219-228.
16. Belousov, A., Belousova, and Voight, B. (1999) Multiple edifice failure, debris avalanches and asssociated eruptions in the Holocene history of Shiveluch volcano, Kamchatka, Russia, *Bull. Volcanol*. **61,** 324-342.

17. Benko, B. and Stead, D. (1998) The Frank Slide: a reexamination of the failure mechanism, *Can. Geotech. Jo*. **35,** 299-311.
18. Bhasin, R. and Kaynia, A.M. In Press. Static and dynamic simulation of a 700-m high rock slope in western Norway. *Eng. Geol*.
19. Birch, G.P., and Warren, C.D. (1996). The cliffs behind the Channel Tunnel workings, *in* C.S. Harris, M.B. Hart, P.M. Varley, and C.D. Warren, (eds.), *Engineering Geology of the Channel Tunnel*, Thomas Telford, London, pp. 76-87.
20. Bishop, K. (1997) Miocene rock-avalanche deposits, Halloran/Silurian Hills area, southeastern California, *Env. Eng. Geosci.* **3**, 501-512.
21. Bjerrum, L. and Jorstad, F.A. (1968). Stability of rock slopes in Norway. Norwegian Geotechnical Institute Publication No. 79, pp. 1-11.
22. Blanc, A., Durville, J-L., Follacci, J-P., Gaudin, B., and Pincent, B. (1987) Methodes de surveillance d'un glissement de terrain de tres grande ampleur : La Clapiere, Alpes Maritimes, France, *Bull. Int. Assoc. of Eng. Geol*., **35**, 37-46.
23. Blikra, L.H., and Nemec, W. (1998) Postglacial colluvium in western Norway: depositional processes, facies and palaeoclimatic record, *Sedimentology* **45**, 909-959.
24. Bogachkin, B.M. and Rogozhin, Y.A. (1994) Rock avalanches on the southern slope of the Greater Caucasus Range produced by the Racha earthquake, *Trans. Russ. Acad. Sci.*, **326**, 29-33.
25. Bovis, M.J. and Evans, S.G. (1995) Rock slope movements along the Mount Currie "fault scarp", southern Coast Mountains, British Columbia, *Can. Jo. Earth Sci.* **32,** 2015 – 2020.
26. Bovis, M.J. and Evans, S.G. (1996) Extensive deformations of rock slopes in southern Coast Mountains, southwest British Columbia, Canada, *Eng. Geol.* **44,** 163-182.
27. Bozzolo, D. and Pamini, R. (1986) Simulation of rock falls down a valley side, *Acta Mech*., **63**, 113-130
28. Bozzolo, D., Pamini, R., and Hutter, K. (1988) Rockfall analysis-a mathematical model and its test with field data, *Proc. 5th Int. Symp. on Landslides*, Lausanne, v. 1, pp. 555-560.
29. Brabb, E.E. and Harrod, B.L. (Editors) (1989) *Landslides: extent and economic significance*. A.A. Balkema, Rotterdam.
30. Bromhead, E.N., Coppola, L., and Rendell, H.M. (1996) Valley-blocking landslide dams in the eastern Italian Alps, *Proc. 7th Int. Symp. on Landslides*, Trondheim, v. 2, pp. 655-660.
31. Bruce, I.G. and Cruden, D.M. (1980) Simple rockslides at Jonas Ridge, Alberta, Canada, *Proc. 3rd. Intl. Symposium on Landslides,* New Delhi, v. 1, p. 185-190.
32. Brückl, E., Brückl, J., and Heuberger, H. (2001) Present structure and prefailure topography of the giant rockslide of Kofels, *Zeits. fur Gletscherkunde und Glazialgeol*., **37,** 49-79.
33. Budetta, P. and Santo, A. (1994). Morphostructural evolution and related kinematics of rockfalls in Campania (southern Italy): a case study, *Eng. Geol.* **36,** 197-210.
34. Burbank, D.W., Leland, J., Fielding, E., Anderson, R.S., Brozovic, N., Reid, M.R., and Duncan, C. (1996) Bedrock incision, rock uplift and threshold hillslopes in the northwestern Himalayas, *Nature* **379**, 505-510.
35. Burchfiel, B.C. (1966) The Tin Mountain landslide, southeastern California, and the origin of megabreccia, *GSA Bull*., **77,** 95-100
36. Burgisser, H.M., Gansser, A., and Pika, J. (1982) Late Glacial lake sediments of the Indus valley area, northwestern Himalayas, *Eclog. Geol. Helv.* **75**, 51-63
37. Butler, R.W.H., and Prior, D.J. (1988) Tectonic controls on the uplift of the Nanga Parbat Massif, Pakistan Himalayas, *Nature* **333,** 247-256.
38. Butler, R.W.H., Owen, L., and Prior, D.J. (1988) Flashfloods, earthquakes and uplift in the Pakistan Himalayas, *Geology Today* **4,** 197-201.
39. Campbell, C.S. (1989) Self-lubrication for long run-out landslides. *Jo. Geol*., **97**, 653-665
40. Campbell, C.S., Cleary, P.W., and Hopkins, M. (1995) Large-scale landslide simulations, global deformation, velocities and basal friction, *Jo. Geophys. Res.* **100B**, 8267-8283.
41. Capra, L. and Macías, J.L. (2002) The cohesive Naranjo debris-flow deposit (10km^3): a dam breakout flow derived from the Pleistocene debris-avalanche deposit of Nevado de Colima volcano (Mexico), *Jo. of Volc. And Geotherm. Res*., **117,** 213-235.
42. Capra, L., Macías, J.L., Scott, K.M., Abrams, M., and Garduño-Monroy, V.H. (2002) Debris avalanches and debris flows transformed from collapses in the Trans-Mexican Volcanic Belt, *Mexico – behaviour, and implications for hazard assessment. Jo. of Volc. and Geotherm. Res.,* **113,** 81-110.

43. Carrasco-Nunez, G., Vallance, J.W., and Rose, W.I. (1993) A voluminous avalanche-induced lahar from Citlaltépetl volcano, Mexico: implications for hazard assessment, *Jo. Volc. Geotherm. Res.* **59**, 35-46
44. Casagli , N., Ermini, L., and Rosati, G. (2002) Determining grain size distribution of the material composing landslide dams in the Northern Appennines: sampling and processing methods, *Eng. Geol.* **69,** 83-97.
45. Cassassa, G. and Marangunic, C. (1993) The 1987 Río Colorado rockslide and debris flow, Central Andes, Chile, *Bull. Ass. Eng. Geol.* **30**, 321-330.
46. Chau, K.T., Wong, R.H.C., and Wu, J.J. (2002) Coefficient of restitution and rotational motions of rockfall impacts, *Int. Jo. Rock Mech. Min. Sci.*, **39**, 69-77.
47. Chau, K.T., Wong, R.H.C., & Lee, C.F. (2003). Rockfall hazard analysis for Hong Kong based on rockfall inventory. *Rock Mech. and Rock Eng.* **36**, 383-408.
48. Chen, T-C., Lin, M-L., and Hung, J-J. (2003) Pseudostatic analysis of Tsao-Ling rockslide caused by Chi-Chi earthquake, *Eng. Geol.* **71,** 31-47.
49. Chigira, M. (1992) Long-term gravitational deformation of rocks by mass rock creep, *Eng. Geol*., **32**, 157-184.
50. Chigira, M. (2000) Geological structures of large landslides in Japan, *Jo. Nepal Geol. Soc.* **22**, 497-504.
51. Chigira, M. and Kiho, K. (1994) Deep-seated rockslide-avalanches preceded by mass rock creep of sedimentary rocks in the Akaishi Mountains, Central Japan, *Eng. Geol*. **38**, 221-230.
52. Choffat, P. (1929) L'écroulement d'Arvel (Villeneuve) de 1922, *Bull. de la Soc. Vaud. Sci. Nat.* **57,** 5-28.
53. Code, J.A. and Sirnhindi, S. (1986) Engineering implications of impoundment of the Upper Indus river, Pakistan, by an earthquake-induced landslide. In R.L. Schuster (Ed.) *Landslide Dams :processes, risk, and mitigation*, Geotechnical Special Publication No. 3, American Society of Civil Engineers, New York, p. 97-109.
54. Cornell, J. (1982*) The great international disaster book,* 3rd. Edition, Charles Scribner, New York, 472 p.
55. Corominas, J. (1996) The angle of reach as a mobility index for small and large landslides, *Can. Geotech. Jo.* **33**, 260-271.
56. Costa, J.E. (1988) Floods from dam failures In V.R. Baker, R.C. Kochel, and P.C. Patton (Editors) *Flood Geomorpholgy*, J. Wiley and Sons, New York, p. 439-463.
57. Costa, J.E. and Schuster, R.L. (1988) The formation and failure of natural dams, *GSA Bull*. **100**, 1054-1068.
58. Crandell, D.R. (1971) *Postglacial lahars from Mount Rainier Volcano, Washington*. United States Geol. Surv. Prof. Paper **677**, 73 p.
59. Crandell, D.R. (1989) Gigantic debris avalanche of Pleistocene age from ancestral Mount Shasta volcano, California, and debris-avalanche hazard zonation, *United States Geol. Surv. Bulletin 1861,* 32 p.
60. Crandell, D.R. and Fahnestock, R.K. (1965) Rockfalls and avalanches from Little Tahoma Peak on Mount Rainier, Washington*, United States Geol. Surv. Bull 1221-A*, 30 p.
61. Crandell, D.R. and Waldron, H.H. (1956) A recent volcanic mudflow of exceptional dimensions from Mt. Rainier, Washington, *Am. Jo. Sci*. **254**, 349-362
62. Crescenti, U., D'Alessandro, L., and Genevois, R. (1987) La Ripa di Montrepiano (Abruzzo): un primo esame delle caratteristiche geomorfologieche in rapporto alla stabilità, *Mem. della Soc. Geol. Ital.* **37**, 775-787.
63. Crescenti, U., Dramis, F., Prestiniinzi, A., and Sorriso-Valvo, M. (1994) Deep-seated gravitational slope deformations and large-scale landslides in Italy, *Dip. di Sci., Univ G. D'Annunzio, Pescara, Italia*, 71 p.
64. Crosta, G.B. and Agliardi, F. (2003) Failure forecast for large rock slides by surface displacement measurements, *Can. Geotech. Jo*., **40**, 176-191.
65. Cruden, D.M. (2000) Some forms of mountain peaks in the Canadian Rockies controlled by their rock structure, *Quat. Int*. **68-71**, 59-75.
66. Cruden, D.M. and Antoine, P. (1984) The slide from Mt. Granier, Isere and Savoie, France, on November 24, 1248, *Proc. 4th Int. Symp. on Landslides*, v.1, p. 475-481.
67. Cruden, D.M. & Hu, X.Q. (1993) Exhaustion and steady state models for predicting landslide hazards in the Canadian Rocky Mountains. *Geomorphology* **8**, 279-285.

68. Cruden, D.M. and Hu, X.Q. (1994) Topples on underdip slopes in the Highwood Pass, Alberta, Canada, *Quart. Jo. Eng. Geol*. **27**, 57-68.
69. Cruden, D.M. and Hu, X.Q. (1996) Hazardous modes of rock slope movement in the Canadian Rockies, *Env. Eng. Geosci*. **2**, 507-516.
70. Cruden. D.M., and Hungr, O. (1986) The debris of the Frank Slide and theories of rockslide-avalanche mobility, *Can. Jo. Earth Sci*. **23**, 425-432.
71. Cruden, D.M. and Lu, Z.Y. (1992) The rockslide and debris flow from Mount Cayley BC in June 1984, *Can. Geotech. Jo*. **29**, 614-626.
72. Cruden, D.M. and Varnes, D.J. (1996) Landslide types and processes. In A.K. Turner and R.L. Schuster (Editors) *Landslides:Investigation and Mitigation*. Transportation Research Board Special Report 247, p. 36-75. National Academy Press, Washington, D.C.
73. Cundall, P.A. (1987) Distinct element models of rock and soil structure, In E.T. Brown (Ed.) *Analytical and Computational Methods in Engineering Rock Mechanics*, Allen and Unwin, London, p. 129-163.
74. Dade, W.B. and Huppert, H.E. (1998) Long-runout rockfalls, *Geology* **26,** 803-806.
75. D'Alessandro, Genevois, R., Berti, M., Urbani, A., and Tecca, P.R. (2002) Geomorphology, stability analyses and the stabilization works on the Montepiano travertinous cliff (Central Italy), In R.J. Allison (ed.) *Applied Geomorphology: Theory and Practice*, John Wiley and Sons, pp. 21-38.
76. Del Prete, M. and Hutchinson, J.N. (1988) La frana di Senise del 267-1986 nel quadro morfologico del verante meridionale della collina Timpone, *Riv. Italiana di Geotec*., **22**, 7-33.
77. Dethier, D.P., and Reneau, S.L. (1996) Lacustrine chronology links late Pleistocene climate change and mass movements in northern New Mexico, *Geology* **24**, 539-542.
78. Dikau, R., Schrott, L., Brunsden, D., and Ibsen, M.-L. (1996) *Landslide Recognition*. J. Wiley, New York, 251 pp.
79. Drew, F. (1875) *The Jummo and KashmirTerritories: a geographical account*. Stanford, London, 568 p.
80. Duperret, A., Genter, A., Mortimore, R.N., Delacourt, B., and De Pomerai, R.D. (2002) Coastal rock cliff erosion by collapse at Puys, France : the role of impervious marl seams within Chalk of NW Europe. *Jo. Coastal Res.* **18**, 52-61.
81. Dussauge, C., Grasso, J-R., & Helmstetter, A. (2003) Statistical analysis of rockfall volume distributions: implications for rockfall dynamics. *Journal of Geophysical Research* **108**, B6, ETG 2-1 to ETG 2-11.
82. Dussauge-Peisser, C., Helmstetter, A., Grasso, J-R., Hantz, D., Desvarreux, P., Jeannin, M., & Giraud, A. (2002) Probabilistic approach to rock fall hazard assessment: potential of historical data analysis. *Natural Hazards and Earth System Sciences* 2: 15-26.
83. Eberhart-Phillips, D., Haeussler, P.J., Freymueller, J.T., Frankel, A.D., Rubin, C.M., Craw, P., Ratchovski, N.A., Anderson, G., Carver, G.A., Crone, A.J., Dawson, T.E., Fletcher, H. Hansen, R., Harp, E.L., Harris, R.A., Hill, D.P., Hreinsdottir, S. , Jibson, R.W., Jones, L.M., Kayen, R., Keefer, D.K., Larsen, C.F., Moran, S.C., Personius, S.F., Plafker, G., Sherrod, B., Sieh, K., Sitar, N., and Wallace, W.K. (2003) The 2002 Denali Fault Earthquake, Alaska: a large magnitude, slip-partitioned event, *Science* **300**, 1113-1118.
84. Eisbacher, G.H., (1979) Cliff collapse and rock avalanches (sturzstroms) in the Mackenzie Mountains, northwestern Canada, *Can. Geot. Jo*. **16**, 309-334.
85. Eisbacher , G.H.and Clague, J.J. (1984) Destructive mass movements in high mountains: hazard and management, *Geological Survey of Canada Paper* 84-16, 230 p.
86. Endo, K., Sumita, M., Machida, M., and Furuichi, M. (1989) The 1984 collapse and debris avalanche deposits of Ontake Volcano, central Japan. In Latter, J.H. (Ed) *Volcanic Hazards*, Springer-Verlag, Berlin, p. 210-229.
87. Enegren, E.G. and Imrie, A.S. (1996) Ongoing requirements for monitoring and maintaining a large remediated rockslide, *Proceedings, 7th. International Symposium on Landslides*, Trondheim, Norway, v. 3, p. 1677-1682.
88. Ermini, L. and Casagli, N. (2003) Prediction of the behaviour of landslide dams using a geomorphological dimensionless index, *Earth Surf. Processes Landforms* **28**, 31-47.
89. Evans, R.S. (1981) An analysis of secondary toppling rock failures-the stress redistribution method. *Quart. Jo. Eng. Geol.* **14**: 77-86.
90. Evans, S.G. (1984) Landslides in Tertiary basaltic successions. *Proceedings, IV International Symposium on Landslides*, Toronto, v.1, 503-510.
91. Evans, S.G. (1989a) Rock avalanche run-up record, *Nature* **340,** 271.

92. Evans (1989b) The 1946 Mount Colonel Foster rock avalanche and associated displacement wave, Vancouver Island, British Columbia. *Can. Geotech. Jo*., **26,** 447-452.
93. Evans, S.G., and Clague, J.J. (1994) Recent climatic change and catastrophic geomorphic processes in mountain environments, *Geomorphology* **10**, 107-128.
94. Evans, S.G., and Clague, J.J. (1998) Rock avalanche from Mount Munday, Waddington Range, British Columbia, Canada, *Landslide News* **11**, 23-25.
95. Evans, S.G. and Clague, J.J. 1999. Rock avalanches on glaciers in the Coast and St. Elias Mountains, British Columbia. In *Slope stability and landslides*, Proceedings, 13th Annual Vancouver Geotechnical Society Symposium, p. 115-123.
96. Evans, S.G. and DeGrafff, J.V. (Editors) (2002) *Catastrophic landslides: effects, occurrences and mechanisms*. Geol. Soc. Am. *Rev. in Eng. Geol*. v. 15, 412p.
97. Evans, S.G. and Hungr, O. (1993) The analysis of rockfall hazard at the base of talus slopes. *Can. Geotech. Jo*. **30**, 620-636.
98. Evans, S.G., Aitken, J.D., Wetmiller, R.J., and Horner, R.B. (1987) A rock avalanche triggered by the October 1985 North Nahanni Earthquake, District of Mackenzie, N.W.T., *Can. Jo. Earth Sci.* **24**, 176-184.
99. Evans, S.G., Clague, J.J., Woodsworth, G.J., and Hungr, O. (1989) The Pandemonium Creek rock avalanche, British Columbia, *Can. Geotech. Jo.* **26**, 427-446
100. Evans, S.G., Couture, R., Locat, J., Hadjigeorgiou, J.,Antoine, P., and Brugnot, G. (1997) Two complex cataclinal slope failures in Paleozoic limestones, Rocky Mountains, Jasper National Park, Alberta, *Proc. 50th Can. Geotech. Conf., Ottawa. Preprint Volume* v. 1, pp. 102-109.
101. Evans, S.G., Hungr, O., and Clague, J.J. (2001) Dynamics of the 1984 rock avalanche and associated debris flow on Mount Cayley, British Columbia, Canada; implications for landslide hazard assessment on dissected volcanoes, *Eng. Geol.* **61**, 29-51.
102. Evans, S.G., Hungr, O. and Enegren, E. G. (1994) The Avalanche Lake rock avalanche, Mackenzie Mountains, Northwest Territories, Canada; description,dating, and dynamics, *Can. Geotech. Jo*. **31**, 749-768.
103. Fauque, L. and Strecker, M.R. (1988) Large rock avalanche deposits (Sturzsröme, sturzstroms) at Sierra Aconquija, northern Sierra Pampeanas, Argentina, *Eclog. Geol. Helv*. **81**, 579-592.
104. Fauque, L. and Tciligharian, P. (2002) Villavil rockslides, Catamarca Province, Argentina, in S.G. Evans and J.V. DeGraff (eds.), *Catastrophic landslides: effects, occurrence, and mechanisms*, Geol. Soc. Am. *Rev. Eng. Geol*., v. XV, pp. 303-324.
105. Finlay, P.J., Mostyn, G.R., and Fell, R. (1999) Landslide risk assessment: prediction of travel distance, *Can. Geot. Jo.* **36**, 556-562.
106. Follacci, J-P. (1987) Les mouvements du versant de la Clapière à Saint-Etienne-de-Tinée (Alpes-Maritimes). *Bull. liason Lab. Pont et Chaussee*, **150**, 31-46.
107. Follacci, J-P., Guardia, P., and Ivaldi, J-P., 1988. Le glissement de la Clapière (Alpes Maritimes, France) dans son cadre géodynamique, *Proc. 5th Int. Symp. on Landslides*, v. 2, pp. 1323-1327.
108. Fort, M. (1987) Sporadic morphogenesis in a continental subduction setting : an example from the Annapurna Range, Nepal Himalaya. *Zeits. fur Geomorph. Suppl.-Bd*. **63**, 9-36.
109. Fort, M. (2000) Glaciers and mass wasting processes: their influence on the shaping of the Kali Gandaki valley (higher Himalaya of Nepal). *Quat. International*, **65/66**, 101-119
110. Fort, M. and Peulvast, J-P. (1995) Catastrophic mass-movements and morphogenesis in the Peri-Tibetan Ranges: examples from West Kunlun, East Pamir, and Ladakh, in O. Slaymaker (ed.) *Steepland Geomorphology* J.Wiley & Sons, New York, pp. 171-198.
111. Fort, M. Burbank, D.W., and Freytet, P. (1989) Lacustrine sedimentation in a semiarid alpine setting: an example from Ladakh, northwest Himalaya, *Quat. Res*., **31**, 332-350.
112. Francis, P.W. and Wells, G.L. (1988) Landsat Thematic Mapper observations of debris avalanche deposits in the Central Andes, *Bull. Volc*., **50**, 258-278.
113. Friedman, S.J. (1997) Rock-avalanche elements of the Shadow Valley Basin, eastern Mojave Desert, California: processes and problems, *Jo. Sed. Res*. **67**, 792-804.S
114. Fritz, H.M., Hager, W.H., and Minor, H-E. (2001) Lituya Bay case: rockslide impact and wave run-up, *Science of Tsunami Hazards* **19**, 3-22.
115. Fuganti, A (1969) Studio geologico di sei grandi frane di roccia nella regione Trentino-Alto Adige, *Mem. del Museo Tridentino di Scienze Naturali*, **17**, 63-128.
116. Fuji, Y. (1969) Frequency distribution of the magnitude of the landslides caused by heavy rainfall. *Journal of the Seismological Society of Japan* **22**, 244-247.

117. Gaziev, E. (1984) Study of the Usoi Landslide in Pamir. *Proc. 4th Int. Symp. on Landslides*, Toronto, v. 1, p. 511-515.
118. Ghirotti, M. (1995) L'Antica frana del M. Borgá e primi resultati del monitoraggio dell'area di prá di salta (Casso, Pn), *Quad. di geologia Applic. Riccione*, **1**, 123-130.
119. Gillon, M.D. and Hancox, G.T. (1992) Cromwell Gorge Landslides – a general overview, *Proc. 6th Int. Symp. on Landslides*, Balkema, Rotterdam, v. 1, 83-120.
120. Giraud, A., Rochet, L., and Antoine, P. (1990) Processes of slope failure in crystallophyllian formations. *Eng. Geol*., **29**, 241-253.
121. Glancy, P.A. and Bell, J.W. (2000) Landslide-induced floodiing at Ophir Creek, *United States Geol. Surv. Prof. Paper* 1617.
122. Glass, J.H. (1896) The great landslip at Gohna, in Garhwal, and the measures adopted to prevent serious loss of life, *Jo. of the Society of Arts*, **44**, 431-445.
123. Glastonbury, J. and Fell, R. (2000) Report on the analysis of "rapid" natural rock slope failures, University of New South Wales School of Civil and Environmental Engineering UNICIV Report No. R-390, 154 p. and Appendices.
124. Govi, M., Gulla, G., and Nicoletti, P.G. (2002) Val Pola rock avalanche of July 28, 1987, in Valtellina (Central Italian Alps), in S.G. Evans and J.V. DeGraff (eds.), *Catastrophic landslides: effects, occurrence, and mechanisms*, Geol. Soc. Am. *Rev. Eng. Geol*., v. XV, pp. 71-89.
125. Griggs, R.F. (1920) The Great Mageik Landslide, *Ohio Jo. of Sci.* **20**, 325-354.
126. Gutenberg, B. and Richter, C.F. (1954) *Seismicity of the Earth*, Princeton University Press, Princeton, 440 p.
127. Guzzetti , F., Cardinali, M., and Reichenbach, P. (1996) The influence of structural setting and lithology on landslide type and pattern, *Env. Eng. Geosci.* **2**, 531-555.
128. Guzzetti, F., Malamud, B.D., Turcotte, D.L., & Reichenbach, P. (2002) Power-law correlations of landslide areas in central Italy, *Earth and Planetary Science Letters* **195**, 169-183.
129. Guzzetti, F., Reichenbach, P. & Wieczorek, G.F. (2003) Rockfall hazard and risk assessment in the Yosemite valley, California, USA, *Natural Hazards and Earth System Sciences* **3**, 491-503.
130. Hancox, G.T. and Perrin, N.D. (1994) Green Lake Landslide: a very large ancient rock slide in Fiordland, New Zealand. *Proc. 7th IAEG Cong*., **v. 3,** 1677-1689.
131. Harp, E.L., Jibson, R.W., Kayen, R.F., Keefer, D.K., Sherrod, B.L., Carver, G.A., Collins, B.D., Moss, R.E.S., and Sitar, N. (2003) Landslides and liquefaction triggered by the M 7.9 Denali Fault earthquake of 3 November 2002, *GSA Today* **13,** 4-10.
132. Harrison, J.V. and Falcon, N.L. (1938) An ancient landslip at Saidmarreh in southwestern Iran, *Jo. Geol*., **46**, 296-309.
133. Hauge, T.A. (1985) Gravity-spreading origin of the Heart Mountain allochton, northwestern Wyoming; GSA Bulletin, **96**, 1440-1456.
134. Hauser, A. (2002) Rock avalanche and resulting debris flow in Estero Parraguirre and Rio Colorado, Región Metropolitana, Chile, in S.G. Evans and J.V. DeGrafff (eds.), *Catastrophic landslides: effects, occurrence, and mechanisms*, Geol. Soc. Am. *Rev. Eng. Geol*., v. XV, pp. 135-148.
135. Havenith, H-B., Strom, A., Jongmans, D., Abdrakhmatov, K., Delvaux, D., and Trefois, P. (2003) Seismic triggering of landslides; Part A: Filed examples from the northern Tien Shan. *Nat. Haz. Earth Syst. Sci.* **3**, 135-149.
136. Heim, Albert. (1932) *Bergsturz und Menschenleben*, Fretz and Wasmuth Verlag, Zurich, 218 p.
137. Heim, Arnold (1948) *Wunderland Peru*, Verlag Hans Huber, Bern, 196 p.
138. Hendron, A.J. and Patton, F.D. (1985) The Vaiont Slide: a geotechnical analysis based on new geological observations of the failure surface: U.S. Army Engineer Waterways Experiment Station, Technical Report GL-85-5, 2 volumes.
139. Henderson, W. (1859) Memorandum on the nature and effects of the flooding of the Indus on 10th August, 1858, as ascertained at Attock and its neighbourhood, *Jo. Asiatic Soc. of Bengal* **28**, 199-219.
140. Hermanns, R.L. and Strecker, M.R. (1999) Structural and lithological controls on large Quaternary rock avalanches (sturzstroms) in arid northwestern Argentina, *GSA Bulletin* **111**, 934-948.
141. Hermanns, R.L., Niedermann, S., Villanueva Garcia, A., Sosa Gomez, J. and Strecker , M.R. (2001) Neotectonics and catstrophic failure of mountain fronts in the southern intra-Andean Puna Plateau, Argentina, *Geology* **29**, 619-623.

142. Hermanns, R.L., Trauth, M.H., Niedermann, S., McWilliams, M. and Strecker, M.R. (2000) Tephrochronologic constraints on temporal distribution of large landslides in northwest Argentina**,** *Jo. of Geol.* **108**, 35-52**.**
143. Hewitt, K. (1968) Records of natural damming and related events in the Upper Indus Basin, *Indus: Jo. of Water and Power Dev. Auth.,* **10,** 11-19.
144. Hewitt, K., (1998) Catastrophic landslides and their effects on the upper Indus streams, Karakoram Himalaya, northern Pakistan, *Geomorphology* **26**, 47-80.
145. Hewitt, K. (1999) Quaternary moraines vs catastrophic rock avalanches in the Karakoram Himalaya, northern Pakistan, *Quat. Res*. **51**, 220-237.
146. Hewitt, K. (2001) Catastrophic rockslides and the geomorphology of the Hunza and Gilgit River valleys, Karakoram Himalaya, *Erdkunde*, **55,** 72-93.
147. Hewitt, K, (2002a) Postglacial landform and sediment associations in a landslide-fragmented river stsytem: the transHimalayan Indus streams, Central Asia, In K. Hewitt, M-L. Byrne, M. English, and G. Young (Eds.) *Landscapes in Transition*, Kluwer Academic Publishers, Dordrecht, p. 63-91.
148. Hewitt, K. (2002b) Styles of rock avalanche depositional complexes conditioned by very rugged terrain, Karakoram Himalaya, Pakistan. In S.G. Evans and J.V. DeGraff (Editors) *Catastrophic Landslides: Effects, Occurrence, and Mechanisms*, Geol. Soc. Am., *Reviews in Engineering Geology*, v. XV, 345- 377.
149. Hoek, E. and Bray, J.W. (1981) *Rock Slope Engineering* 3rd Ed. Inst. Min. Metall., London,
150. Holland, T.H. (1894) Report on the Gohna Landslip, Garhwal. *Records Geol. Surv. of India* **27,** 55-65.
151. Hovius, N., Stark, C.P., and Allen, P.A. (1997) Sediment flux from a mountain belt derived by landslide mapping, *Geology* **25**, 231-234.
152. Hovius, N., Stark, C.P., Tutton, M.A., and Abbott, L.D., (1998) Landslide-driven drainage network evolution in a pre-steady-state mountain belt: Finisterre Mountains, Papua New Guinea, *Geology* **26**, 1071-1074.
153. Hsu, K.J. (1975) Catastrophic debris streams (sturzstroms) generated by rockfalls, *GSA Bull.* **86**, 129-140.
154. Hu, X.Q. and Cruden, D.M. (1993) Buckling deformation in the Highwood Pass, Alberta, Canada, *Can. Geotech. Jo.* **30**, 276-286.
155. Huder, J. (1976) Creep in Bunder Schist, *Laurits Bjerrum Memeorial Volume*, Norwegian Geotechnical Institute, Oslo, p. 125-153.
156. Hung, J-J., Lee, C-T., and Lin, M-L. (2002) Tsao-Ling rockslides, Taiwan, in S.G. Evans and J.V. DeGraff (eds.), *Catastrophic landslides: effects, occurrence, and mechanisms*, Geol. Soc. Am. *Rev. Eng. Geol*., v. XV, pp. 91-115.
157. Hungr, O. (1995) A model for the runout analysis of rapid flow slides, debris flows, and avalanches, *Can. Geotech. Jo.* **32**, 610-623.
158. Hungr, O. and Evans, S.G. (1988) Engineering evaluation of fragmental rockfall hazards. *Proceedings, V International Symposium on Landslides*, v. **1**, p. 685-690.
159. Hungr, O. and Evans, S.G. (1996) Rock avalanche runout prediction using a dynamic model. *Procceedings, 7th International Symposium on Landslides*, Trondheim, Norway, v. 1, p. 233-238.
160. Hungr, O. and Evans, S.G. (1997) A dynamic model for landslides with changing mass. *Proceedings of International Association of Engineering Geology Symposium on Engineering Geology and the Environment*, Athens, Greece, v. 1, p. 719-724.
161. Hungr, O., Evans, S.G., and Hazzard, J. (1999) Magnitude and frequency of rock falls and rock slides along the main transportation corridors of southwestern British Columbia, *Can. Geotech. Jo*. **36**, 224-238
162. Hungr, O., Dawson, R.F., Kent, A., Campbell, D., and Morgenstern, N.R. (2002) Rapid flow slides of coal-mine waste in British Columbia, Canada, in S.G. Evans and J.V. DeGraff (eds.), *Catastrophic landslides: effects, occurrence, and mechanisms*, Geol. Soc. Am. *Rev. Eng. Geol*., v. XV, pp. 191-208.
163. Hungr, O., Evans, S.G., Bovis, M.J., and Hutchinson, J.N. (2001) A review of the classification of landslides of the flow type, *Env. Eng. Geosci.* **7**, 221-238.
164. Hutchinson , J.N. (1971). Field and laboratory studies of a fall in Upper Chalk cliffs at Joss Bay, Isle of Thanet. In *Stress-Strain behaviour of soils*, Proceedings, Roscoe Memorial Symposium, Cambridge, pp. 692-706.
165. Hutchinson, J,N, (1987) Mechanisms producing large displacements in landslides on pre-existing shears, *Mem. Geol. Soc. of China* **9**, 175-200.

166. Hutchinson, J.N. (1988) General report : morphological and geotechnical parameters of landslides in relation to geology and hydrogeology, *Proceedings of the 5th International Symposium on Landslides*, Lausanne, Switzerland, v. 1, 3-35.
167. Hutchinson, J.N. (1995) Deep-seated mass movements on slopes, *Mem. Soc. Geol. It*., **50**: 147-164
168. Hutchinson, J.N. (2002) Chalk flows from the coastal cliffs of northwest Europe, in S.G. Evans and J.V. DeGraff (eds.), *Catastrophic landslides: effects, occurrence, and mechanisms*, Geol. Soc. Am. Rev. Eng. Geol., v. XV, pp. 257-302.
169. Hutchinson, J.N. and Kojan, E. (1975) The Mayunmarca Landslide of 25th April 1974, Peru, *Report Ser. No. 3124/RMO..RD/SCE*, UNESCO, Paris.
170. Imrie, A.S. and Moore, D.P.(1997) BC Hydro's approach to evaluating reservoir slope stability from a risk perspective, In D.M. Cruden and R. Fell (Editors) *Landslide Risk Assessment*, A.A. Balkema, Rotterdam, pp. 215-226.
171. Imrie, A.S., Moore, D.P., and Enegren, E.G. (1992) Performance and maintenance of the drainage system at Downie Slide, *Proceedings, 6th International Symposium on Landslides*, Christchurch, New Zealand, v. 1, p. 751-757, A.A. Balkema, Rotterdam.
172. Ishida, T., Chigira, M., and Hibino, S. (1987) Application of the Distinct Element Method for analysis of toppling observed on a fissured rock slope. *Rock Mech. and Rock. Eng*. **20**, 277-283.
173. Iverson, R.M., Reid, M.E., and LaHusen, R.G. (1997) Debris-flow mobilization from landslides, *Ann. Rev. Earth Plan. Sci.*, **25,** 85-138.
174. Jackson, L.E. (2002) Landslides and landscape evolution in the Rocky Mountains and adjacent Foothills area, southwestern Alberta, Canada, in S.G. Evans and J.V. DeGraff (eds.), *Catastrophic landslides: effects, occurrence, and mechanisms*, Geol. Soc. Am. *Rev. Eng. Geol*., v. XV, pp. 325-344.
175. Janda, R.J., Scott, K.M., Nolan, K.M., and Martinson, H.A. (1981) Lahar movement, effects, and deposits, In Lipman, P.W. and Mullineaux, D.R. (Editors) The 1980 eruptions of Mount St Helens, Washington, *United States Geol. Surv., Prof. Paper* **1250,** p. 461-478.
176. Jing, L. (2003) A review of techniques, advances and outstanding issues in numerical modelling for rock mechanics and rock engineering, *Int. Jo. of Rock Mech. and Mining Sci.,* **40**, 283-353.
177. Johnson, R.W. (1987) Large-scale volcanic cone collapse: the 1888 slope failure of Ritter volcano, and other examples from Papua New Guinea, *Bull. Volcanol*., **49**, 669-679.
178. Jones, B.L., Chinn, S.S.W., and Brice, J.C. (1984) Olokele rock avalanche, island of Kauai, Hawaii, *Geology* **12**, 209-211.
179. Jorstad, F. (1968) Waves generated by landslides in Norwegain fjords and lakes. Norwegian Geotechnical Institiute Publication No. 69, p. 13-32.
180. Kalkani, E.C. and Piteau, D.R. (1976) Finite element analysis of toppling failure at Hell's Gate Bluffs, British Columbia, *Bull. Assoc. Eng. Geol*., **13,** 315-327
181. Keefer, D.K., (1984) Landslides caused by earthquakes, *Geol. Soc. Am. Bull*. **95**, 406-421.
182. Keefer, D.K., (1994) The importance of earthquake-induced landslides to long-term slope erosion and slope-failure hazards in seismically active regions, *Geomorpholgy* **10**, 265-284.
183. Keefer, D.K. (2002) Investigating landslides caused by earthquakes – a historical review, *Surv. in Geophysics* **23**, 473-510.
184. Kerle, N. and van Wyk de Vries, B., (2001) The 1998 debris avalanche at Casita volcano, Nicaragua – investigation of structural deformation as the cause of slope instability using remote sensing, *Jo. Volc. Geotherm. Res*. **105**, 49-63.
185. Kiersch, G.A. (1964) Vaiont reservoir disaster, *Civil Engineering, ASCE* **34**: 32-39
186. Kilburn, C.R.J., and Sorensen, S-A. (1998) Runout lengths of sturzstroms: the control of initial conditions and of fragment dynamics *Jo. Geophys. Res.* **103B**, 17877-17884.
187. Kimber, O.G., Allison, R.J., and Cox, N.J. (1998) Mechanisms of failure and slope development in rock masses. *Trans. Inst. Br. Geogr*., **NS 23**, 353-370.
188. King, J.., Loveday, I., and Schuster, R.L. (1989) The 1985 Bairaman landslide dam and resulting debris flow, Papua New Guinea, *Quat. Jo. Eng. Geol.* **22**, 257-270.
189. Kjartansson, G. (1967) The Steinsholtshlaup, central-south Iceland on January 15th , 1967, *Jokull* **17**, 249-262.
190. Kobayashi, Y., Harp, E.L., and Kagawa, T. (1990) Simulation of rockfalls triggered by earthquakes, *Rock Mech. and Rock. Eng*. **23**, 1-20.
191. Kohlbeck, F., Scheidegger, A.F. and Sturgul, J.R. (1979) Geomechanical model of an alpine valley. *Rock Mech*., **12**, 1-14.
192. Kolderup, N-H. (1955) Raset I Modalen 14. August 1953, *Norsk Geol. Tidssk*. **34**, 211-217.

193. Korup, O. (2002) Recent research on landslide dams – a literature review with special attention to New Zealand. *Prog. in Phys. Geog*., **26**, 206-235.
194. Krahn, J. and Morgenstern, N.R. (1976) Mechanics of the Frank slide. *In* Rock Engineering for Foundations and Slopes; American Society of Civil Engineers, v. 1, p. 309-331.
195. Krieger, M.H. (1977) Large landslides, composed of megabreccia, interbedded in Miocene basin deposits, southeastern Arizona, *United States Geol. Surv. Prof. Paper* 1008, 25 p.
196. Latter, J.H. (1981) Tsunamis of volcanic origin: summary of causes, with particular reference to Krakatoa, 1883, *Bull. Volcanol*. **44**, 467-499.
197. Lee, K.L. and Duncan, J.M. (1975) Landslide of April 25, 1974 on the Mantaro River, Peru. *National Acad. Sci*., Washington, DC, 72 p.
198. Legros, F. (2002) The mobility of long run-out landslides, *Eng. Geol*. **63,** 301-331.
199. Lehmann, O. (1926) Die verheerungen in der Sandlinggruppe (Salzkammergut), *Akad. Der Wiss. In Wien, Denk*. **100**, 259-299.
200. Leoniv, N.N. (1960) The Khait, 1949 earthquake and geological conditions of its ocurrence. *Izvestia of the Academy of Sciences of the USSR, Geophysical Series*, No 3, 409-424.
201. Longwell, C.R. (1951) Megabreccia developed downslope from large faults, *Am. Jo. Sci*., **249**, 343-355.
202. Lopez, D.L. and Williams, S.N. (1993) Catastrophic volcanic collapse: relation to hydrothermal processes, *Science* **260**, 1794-1796.
203. Li, T. and Wang, S. (1992) *Landslide hazards and their mitigation in China*, Science Press, Beijing, 84 pp.
204. Li, T., Schuster, R.L., and Wu, J. (1986) Landslide dams in south-central China, R.L. Schuster (ed.) *Landslide Dams:processes, risk, and mitigation,* Geotechnical Special Publication No. 3, American Society of Civil Engineers, New York, p. 146-162.
205. Lliboutry, L., Morales, B., Pautre, A. and Schneider, B. (1977) Glaciological problems set by the control of dangerous lakes in Cordillera Blanca, Peru. 1. Historical failures of morainic dams, their causes and prevention, *Jo. of Glaciol*., **18**, 239-254.
206. Mader, C.L. (1999) Modelling the 1958 Lituya Bay mega-tsunami, *Science of Tsunami Hazards* **17**, 57-67.
207. Major, J.J. and Newhall, C.G. (1989) Snow and ice perturbation during historical volcanic eruptions and the formation of lahars and floods, *Bull. Volcanol.* **52, 1**-27.
208. Martin, C.D. and Kaiser, P.K. (1984) Analysis of a rock slope with internal dilation. *Can Geotech. Jo*. **21**, 605-620.
209. Martino, S., Prestininzi, A. and Scarascia-Mugnozza, G. (2001) Mechanisms of deep seated gravitational deformations: parameters from laboratory testing for analogical and numerical modeling, in P. Sarkka P. Eloranta (eds.) *Rock mechanics – a challenge for society*, Balkema, Rotterdam, p. 137-142.
210. Mason, K. (1929) Indus Floods and Shyok Glaciers, *Himal. Journal* **1**, 10-29.
211. Matsukura, Y. (2001) Rockfall at Toyohama Tunnel, Japan, in 1996: effect of notch growth on instability of a coastal cliff, *Bull. Eng. Geol. Env*. **60**, 285-289.
212. McCalpin, J.P. (1999) Criteria for determining the seismic significance of sackungen and other scarplike landforms in mountainous regions. Appendix A, p. A-122 to A-142 in *Techniques for identifying faults and determining their origins*. U.S. Nuclear Regulatory Commission NUREG/CR-5503.
213. McCalpin, J.P. and Irvine, J.R. (1995) Sackungen at the Aspen Highlands ski area, Pitkin County, Colorado, *Env. Eng. Geosci.* **1**, 277-290.
214. McConnell, R.G. and Brock, R.W. (1904) Report on the Great Landslide at Frank, Alberta, *Annual Report of the Department of Interior for the year 1902-1903, Part VIII*, 17 p.
215. McGuire, W.J. (1996). Volcano instability; a review of contemporary themes. In McGuire, W.J., Jones, A.P. and Neuberg, J. (Editors) 1996. *Volcano instability on the earth and other planets*. Geological Society of London Special Publication No. 11, p. 1-23.
216. McSaveney, M.J. (1978) Sherman Glacier rock avalanche, Alaska, U.S.A. in B. Voight (ed.) *Rockslides and avalanches, 1. Natural Phenomena,* Elsevier, Amsterdam, p.197-258.
217. McSaveney, M.J. (2002) Recent rockfalls and rock avalanches in Mount Cook National Park, New Zealand, in S.G. Evans and J.V. DeGraff (eds.), *Catastrophic landslides: effects, occurrence, and mechanisms*, Geol. Soc. Am. *Rev. Eng. Geol*., v. XV, pp. 35-70.

218. Meidal, K.M. and Moore, D.P. (1996) Long-term performance of instrumentation at Dutchman's Ridge, *Proceedings, 7th. International Symposium on Landslides*,Trondheim, Norway, v. 3, p. 1565-1570.
219. Melekestsev, I.V., and Braitseva, O.A. (1988) Gigantic collapses on volcanoes, *Volcanology and Seis-mology* **6**, 495-508 (in Russian).
220. Miller, D.J. (1960) Giant waves in Lituya Bay, Alaska, *United States Geol. Surv. Prof. Paper* 354-C, p. 51-86.
221. Montadon, F. 1933. Chronologie des grands éboulements alpins du début de l'ère chrétienne à nos jours. *Matériaux pour l'étude des calamités*, **32**, 271-340.
222. Moore, D.P. (1990) Stabilization of Dutchman's Ridge, *Geotechnical News*, **8**, 47.
223. Moore, D.P. and Imrie, A.S. (1995) Stabilization of Dutchman's Ridge, *Proceedings of 6th International Symposium on Landslides*, Christchurch, New Zealand, v.3, p. 1783-1788.
224. Moore, D.P., Ripley, B.D., and Groves, K.L. (1992) Evaluation of mountainslope movements at Wahleach; in *Geotechnique and natural hazards* Bitech Publishers, Vancouver, B.C. p. 99-107.
225. Moriwaki, H., Yazaki, S., and Oyagi, N. (1985) A gigantic debris avalanche and its dynamics at Mount Ontake caused by the Nagano-ken-seibu earthquake, 1984. *Proc. 4th Int. Conf. Field Workshop on Landslides*, Tokyo, p. 359-364.
226. Morris, T.H. and Hebertson, G.F. (1996) Large-rock avalanche deposits, eastern Basin and Range, Utah: emplacement, diagenesis, and economic potential, *AAPG Bulletin* **80**, 1135-1149.
227. Mothes, P.A., Hall, M.L., and Janda, R.J. (1998) The enormous Chillos Valley Lahar: an ash-flow-generated debris flow from Cotopaxi Volcano, Ecudaor, *Bull. Volcanol*. **59,** 233-244.
228. Muller, L. (1964) The rock slide in the Vaiont valley, *Rock Mech. and Eng. Geol*., **6,** 148-212.
229. Naranjo, J.A. and Francis, P. (1987) High velocity debris avalanche at Lasstarria volcano in the north Chilean Andes, *Bull. Volc*. **49**, 509-514.
230. Nichol, S.L., Hungr, O., and Evans, S.G. (2002) Large-scale brittle and ductile toppling of rock slopes, *Can. Geotech. Jo*. **39**, 773-788.
231. Nicoletti, P.G. and Parise, M. (1996) Geomorphology and kinematics of the Conturrana rockslide-debris flow (NW Sicily), *Earth Surf. Proc .and Landforms*, **21,** 875-892.
232. Niederer, J., (1941) Der Felssturz am Flimserstein. *Jahresbericht der Naturforschenden Gesellschaft Graubünden,* Chur
233. Nikonov, A.A., and Shebalina, T.Y. (1979) Lichenometry and earthquake age determination in central Asia, *Nature* **280**, 675-677.
234. Norrish, N.I. and Wyllie, D.C. (1996) Rock slope stability analysis. In A.K. Turner and R.L. Schuster (Editors) *Landslides:investigation and mitigation,* Special Report 247 Tran. Res. Bd., Nat. Res. Council, National Academy Press, Washington, p. 391-425
235. Noverraz , F. (1996) Sagging or deep-seated creep: fiction or reality? *Proc. 7th International Symposium on Landslides,* Trondheim, Norway, p, 821-828, A.A. Balkema, Rotterdam
236. Ogawa, T. and Homma, F. (1926) The geology of the Unzen Volcanoes, Pan-*Pac. Sci. Congr. Guidebook for Excursion E-1, 3, 4*, 30 p.
237. Ohmori, H. and Hirano, M. (1988) Magnitude, frequency and geomorphological significance of rocky mud flows, landcreep, and the collapse of steep slope, *Zeits für Geomorph, Suppl. –Bnd* **67,** 55-65.
238. Orombelli, G. and Porter, S.C. (1988) Boulder deposit of upper Val Ferret (Courmayeur, Aosta valley) : deposit of a historic giant rockfall and debris avalanche or a late-glacial moraine ? *Eclog. Geol. Helv.* **81**, 365-371.
239. Osipov, V.I., Mamaev, Yu.A. (1998) Peculiarities of formation and structure of large-scale blockages in mountain valleys. *Geoecology, Engineering Geology, Hydrogeology, Geocryology*, **6**, 94-99 (in Russian).
240. Ota, K. (1969) Study on the collapses in the Mayu-yama, *Sci. Rpt. Shimabara Volc. Obs., Fac. Sci., Kyushu University*, **5**: 6-35 (in Japanese)
241. Owen, L. (1989) Neotectonics and glacial deformation in the Karakoram Mountains and Nanga Parbat Himalaya, *Tectonophysics*, **163**, 227-265.
242. Owen, L. A. (1996) Quaternary lacustrine deposits in a high-energy semi-arid mountain environment, Karakoram Mountains, northern Pakistan, *Jo. Quat. Sci.* **11**, 461-483.
243. Paul, S.K., Bartarya, S.K., Rautela, P., and Mahajan, A.K. (2000) Catastrophic masss movement of 1998 monsoons at Malpa in Kali Valley, Kumaun Himalaya (India), *Geomorphology* **35**, 169-180.
244. Pedersen, S.A.S., Larsen, L.M., Dahl-Jensen, T., Jepsen, H.F., Pedersen, G.K., Nielsen, T., Pedersen, A.K., von Platen-Hallermud, F., and Weng, W. (2002) Tsunami-generating rock fall and landslide on

the south coast of Nuussuaq, central West Greenland, *Geology of Greenland Survey Bulletin*, **191**, 73-83.

245. Pelletier, J.D., Malamud, B.D., Blodgett, T., & Turcotte, D.L. (1997) Scale-invariance od soil moisture variability and its implications for the frequency-size distribution of landslides, *Eng. Geol.* **48**, 255-268.
246. Pfeiffer, T.J. and Bowen, T.D. (1989) Computer simulation of rockfalls, *Bull. Assoc. Eng. Geol*. **26,** 135-146.
247. Philip, H. and Ritz, J-F. (1999) Gigantic paleolandslide associated with active faulting along the Bogd fault (Gobi-Altay, Mongolia), *Geology* **27**, 211-214.
248. Plafker, G. (1968) Source areas of the Shattered Peak and Pyramid Peak Landslides at Sherman Glacier. In *The Great Alaska Earthquake of 1964.* v. 3, p. 374-382. National Academy of Sciences, Washington, D.C.
249. Plafker, G. and Eriksen, G.E. (1978) Nevados Huascarán avalanches, Peru. In B. Voight (Ed.) *Rockslides and Avalanches v. 1,* Elsevier, Amsterdam, p. 277-314.
250. Plafker, G. and Eyzaguirre, V.R. (1979) Rock avalanche and wave at Chungar, Peru. In B. Voight (Ed.) *Rockslides and Avalanches, v. 2. Engineering Sites*, Elsevier, Amsterdam, p. 269-279
251. Poisel, R. (1998) Kippen, Sacken, Gleiten, *Felsbau*, **16,** 135-140.
252. Porter, S.C. and Orombelli, G. (1980) Catastrophic rockfall of September 12, 1717 on the Italian flank of the Mont Blanc Massif, *Zeits. fur Geomorph*. **24**, 200-218.
253. Porter, S.C. and Orombelli, G. (1981) Alpine rockfall hazards, *American Scientist*, **69**, 67-75.
254. Poschinger, A. von. (2002) Large rockslides in the Alps: A commentary on the contribution of G. Abele (1937-1994) and a review of some recent developments, in S.G. Evans and J.V. DeGraff (eds.), *Catastrophic landslides: effects, occurrence, and mechanisms*, Geol. Soc. Am. *Rev. Eng. Geol*., v. XV, pp. 237-255.
255. Post, A. (1967) Effects of the March 1964 Alaska Earthquake on Glaciers, *United States Geol. Surv. Prof. Paper* 544-D, 42 p.
256. Preobrajensky, J. (1920) The Usoi Landslide, *Geol. Comm., Papers on Applied Geol., 14*, 21 p. (In Russian)
257. Pritchard, M.A. and Savigny, K.W. (1990) Numerical modeling of toppling, *Can. Geotech. Jo*., **27**, 823-834.
258. Pritchard, M.A and Savigny, K.W. (1991) The Heather Hill landslide: an example of a large scale toppling failure in a natural slope, *Can. Geotech. Jo*. **28**, 410-422
259. Read, S.A.L., Beetham, R.D., and Riley, P.B. (1992) Lake Waikaremoana barrier – a large landslide dam in New Zealand, *Proc. 6th Intern. Symposium on Landslides*, Christchurch, New Zealand, v. 2, pp. 1481-1487, Balkema, Rotterdam.
260. Reid, M.E., Christian, S.B., and Brien, D.L. (2000) Gravitational stability of three-dimensional stratovolcano edifices, *J. Geophys. Res.* **105**, 6043-6056.
261. Reid, M.E., Sisson, T.W., and Brien, D.L. (2001) Volcano collapse promoted by hydrothermal alteration and edifice shape, Mount Rainier, Washington, *Geology* **29**, 779-782.
262. Reneau, S.L., and Dethier, D.P., (1996) Late-Pleistocene landslide-dammed lakes along the Rio Grande, White Rock Canyon, New Mexico, *GSA Bull*. **108,** 1492-1507.
263. Riemer, W., Locher, T., and Nunez, I. (1988) Mechanics of deep seated mass movements in metamorphic rocks in the Ecuadorian Andes, *Proceedings of the 5th International Symposium on Landslides*, Lausanne, Switzerland, v. 1, 307-310.
264. Rodriguez, C.E., Bommer, J.J., and Chandler, R.J. (1999) Earthquake-induced landslides: 1980-1997, *Soil Dyn. and Earthquake Eng*. **18**, 325-346.
265. Sartori, M., Baillifard, Jaboyedoff, M., and Rouiller, J-D. (2003) Kinematics of the 1991 Randa rockslides (Valais, Switzerland) *Nat. Haz. and Earth Syst. Sci*., **3**, 423-433
266. Sassa, K. (1988) Geotechnical model for the motion of landslides (Special lecture). *Proceedings, 5th International Symposium on Landslides*, Lausanne, Switzerland, v. 1, p. 37-56.
267. Sassa, K. (Editor) (1999) *Landslides of the world*. Kyoto University Press, 413 pp.
268. Savage, S.B. and Hutter, K. (1991) The dynamics of avalanches of granular materials from initiation to runout. Part 1. Analysis, *Acta Mech.* **86**, 201-223.
269. Scarpa, R. and Tilling, R.I. (Editors) (1996) *Monitoring and Mitigation of Volcano Hazards,* Springer-Verlag, Berlin. 841 pp.
270. Scheidegger, A.E., (1973) On the prediction of the reach and velocity of catastrophic landslides. *Rock Mechanics*, **5**, 231-236.

271. Scheko, A.I. and Lekhatinov, A.M. (1970) Current state of the Usoi Blockage and tasks of future studies. In *Materials of Scientific-technical meeting on the problems of study and forecast of the mudflows, rockfalls and landslides*, Dushanbe, 219-223 (in Russian)
272. Schuster, R.L. (2002) Usoi landslide dam, southeastern Tajikistan, *Proc. Int. Symp. on Landslide Risk Mitigation and Protection of Cultural and Natural Heritage*, Kyoto, p. 489-505
273. Schuster, R.L., Logan, R.L., and Pringle, P.T., (1992) Prehistoric rock avalanches in the Olympic Mountains, Washington, *Science* **258**, 1620 – 1621.
274. Scott, K.M. (1988) Origins, behaviour and sedimentology of lahars and lahar-runout flows in the Tooutle-Cowlitz river system, *United States Geol. Surv. Prof. Paper* 1447-A, 74 p.
275. Scott, K.M. (2000) Precipitation-triggered debris flow at Casita Volcano, Nicaragua: implications for mitigation strategies in volcanic and tectonically active steeplands, in G.F. Wieczorek and N.D. Naeser (eds.) *Debris-flow hazards mitigation: mechanics, prediction and assessment*, A.A. Balkema, Rotterdam, p. 3-13
276. Scott, K.M., Macías, J.L., Naranjo, J.A., Rodriguez, S., and McGeehin, J.P. (2001) *Catastrophic debris flows transformed by landslides in volcanic terrains: mobility, hazard assessment, and mitigation strategies*. *United States Geol. Surv. Prof. Paper* 1630, 67 p.
277. Selli, R. and Trevisan, L. (1964) Caratteri e interpretazione della frana del Vaiont, *Giornale di Geologia* **32**, 7-104.
278. Semenza, E. and Ghirotti, M. (1998) Vaiont-Longarone 34 Anni Dopo La Catastrophe. *Annali dell'Univsita di Ferrara (Nuovo Serie) Scienze della Terra* **7**, 63-94.
279. Semenza, E. and Ghirotti, M. (2000) History of the 1963 Vaiont slide: the importance of geological factors, *Bull. Eng. Geol. Env.* **59**, 87-97.
280. Sevilla, J.H. (1994) The Josefina landslide and its implications in the electrical service for the Republic of Ecuador; *Proceedings, 7th International Congress, International Association of Engineering Geology*, Lisbon, v. 3, p. 1801-1810.
281. Shang,Y., Yang, Z., Li, L., Liu, D., Liao, Q. and Wang, Y. (2003) A super-large landslide in Tibet in 2000 : background, occurrence, disaster, and origin, *Geomorphology* **54**, 225-243.
282. Sharpe, C.F.S. (1938) *Landslides and related phenomena*, Columbia University Press, New York, 137 pp.
283. Sheridan, M.F., Bonnard, C., Carreno, R., Siebe, C., Strauch, W., Navarro, M., Calero, J.C., and Trujillo, N.B. 1999. Report on the 30 October 1998 Rock Fall/ Avalanche and breakout flow of Casita Volcano, Nicaragua, triggered by Hurricane Mitch, *Landslide News*, v. 12, p. 2-4.
284. Shpilko, G.A. (1915) New data on the Usoi blockage and the Sarez Lake, *Proc. of the Turkestan Department of Russian Geographical Society*, **11**, 11-17 (in Russian).
285. Siebert, L. (1984) Large volcanic debris avalanches: characteristics of source areas, deposits, and associated eruptions, *Jo. Volc. Geotherm. Res*. **22**, 163-197.
286. Siebert, L. (1996) Hazards of large volcanic debris avalanches and associated eruptive phenomena, in R. Scarpa and R.I. Tilling (eds.) *Monitoring and mitigation of volcano hazards*, Springer-Verlag, Berlin, p. 541-57.
287. Siebert, L. (2002) Landslides resulting from structural failure of volcanoes, in S.G. Evans and J.V. DeGraff (eds.), *Catastrophic landslides: effects, occurrence, and mechanisms*, Geol. Soc. Am. Rev. Eng. Geol., v. XV, pp. 209-235.
288. Siebert, L., Beget, J.E., and Glicken, H. (1995) The 1883 and late-prehistoric eruptions of Augustine volcano, Alaska, *Jo. of Volc. and Geotherm. Res.* **66**, 367-395.
289. Siebert, L., Glicken, H., and Ui, T. (1987) Volcanic hazards from Bezymianny- and Bandai-type eruptions, *Bull. Volcanol*. **49,** 435-459.
290. Singh, N.K. & Vick, S.G. (2003) Probabilistic rockfall hazard assessment for roadways in mountainous terrain. *Proceedings, 3rd Canadian Conference on Geotechnique and Natural Hazards,* Canadian Geotechnical Society, Edmonton, p. 253-260.
291. Slingerland, R.L. and Voight, B. (1979) Occurrences, properties and predictive models of landslide-generated impulse waves. In B. Voight (Ed.) *Rockslides and avalanches v. 2*, p. 317-397, Elsevier, Amsterdam.
292. Solonenko, V.P. (1970) Scars on the Earths' face, *Priroda (Nature)*, **9**, 17-25 (in Russian).
293. Solonenko, V.P. (1972) Seismogenic destruction of mountain slopes, *Proc. Int. Geol. Congr., Section 13*, Montreal, p. 284-290.
294. Solonenko, V.P. (1977) Landslides and collapses in seismic zones and their prediction, *Bull. Int. Assoc. Eng. Geol*., **15**, 4-8 .
295. Sousa, J, and Voight, B. (1991) Continuum simulation of flow failures, *Geotechnique*, **41,** 515-538.

296. Stead, D. and Eberhardt, E. (1997) Developments in the analysis of footwall slopes in surface coal mining, *Eng. Geol.* **46**, 41-61.
297. Steidl, A. and Riedmuller, G. (2003) Deep-seated gravitational slope deformation – a case study. *Felsbau* 21: 55-61.
298. Stoopes, G.R. and Sherida\n, M.F. (1992) Giant debris avalanches from the Colima Volcanic Complex, Mexico: implications for long-runout landslides (>100 km) and hazard assessment, *Geology* **20**, 299-302.
299. Strecker, M.R., and Marrett, R. (1999) Kinematic evolution of fault ramps and its role in development of landslides and lakes in the northwestern Argentine Andes, *Geology* **27,** 307-310.
300. Strom, A.L. (1994a) Mechanism of stratification and abnormal crushing of rockslide deposits. *Proceedings, 7th International Association of Engineering Geology Congress*, Lisbon, Portugal, v. 3, p. 1287-1295.
301. Strom, A.L. (1994b) Formation of structure of large rockslide deposits, *Geoecology, Engineering Geology, Hydrogeology, Geocryology*., No 5, 64-77 (in Russian).
302. Strom, A.L. (1996) Some morphological types of long-runout rockslides: effect of the relief on their mechanism and on the rockslide deposits distribution. In K. Senneset (ed.) Landslides, *Proceedings, 7th International Symposium on Landslides*, Trondheim, Norway, p. 1977-1982.
303. Strom, A.L. (1998) Giant ancient rockslides and rock avalanches in the Tien Shan Mountains, Kyrgyzstan, *Landslide News*, **11**, 20-23.
304. Sugai, T., Ohmori, H., & Hirano, M. (1994) Rock control on magnitude-frequency distribution of landslides. *Transactions Japanese Geomorphological Union* **15**, 233-251.
305. Suklje, L. and Vidmar, S. (1961) A landslide due to long term creep. *Proc. 5th Int. Conf. Soil Mech. and Found. Eng.*, **v. 2**, 727-735.
306. Suwa, H. (1991) Visually observed failure of a rock slope in Japan, *Landslide News*, **5,** 8-10.
307. Tabor, R.W. (1971) Origin of ridge top depressions by large-scale creep in the Olympic Mountains, Washington. *GSA Bulletin* **82,** 1811-1822.
308. Terzaghi, K. (1960) Storage dam founded on landslide debris, *Journal of the Boston Society of Civil Engineers*, **47,** 64-94.
309. Thorsen, G.W. (1989) Splitting and sagging of mountains, *Washington Geology*, **17,** 3-13.
310. Thompson, S.C., Clague, J.J., and Evans, S.G. (1997) Holocene activity of the Mt. Currie scarp, Coast Mountains, British Columbia, and implications for its origin. *Environmental and Engineering Geoscience*, **3,** 329-348.
311. Tika, T.E. and Hutchinson, J.N. (1999) Ring shear tests on soil from the Vaiont landslide slip surface, *Geotechnique* **49,** 59-74.
312. Tommasi, P. and Galadini, F. (1996) Rock slides and buckling phenomena on a homoclinal mountain slope in south-eastern Alps (Italy) *Proc. 7th Int. Symp. on Landslides*, Trondheim, v. 2, 1391-1396, Balkema, Rotterdam.
313. Trauth, M.H., Alonso, R.A., Haselton, K.R., Hermanns, R.L. and Strecker, M.R. (2000) Climate change and mass movements in the Argentine Andes, *Earth Planet. Sci. Lett.* **179,** 243-256.
314. Trauth, M.H., Bookhagen, B., Marwan, N., and Strecker, M. (2003) Multiple landslide clusters record Quaternary climate changes in the northwestern Argentine Andes, *Palaeogeog., Palaeoclim., Palaeoec*., **194,** 109-121.
315. Trunk, F.J., Dent, J.D., and Lang, T.E. (1986) Computer modeling of large rock slides, *Jo. Geotech. Eng*., **112**, 348-360
316. Tsuji, Y. and Hino, T. (1993) Damage and inundation height of the 1792 Shimabara landslide tsunami along the coast of Kumamoto Prefecture, Bulletin of the Earthquake Research Institute, University of Tokyo, **68**, 91-176.
317. Ui, T., Yamamoto, H., and Suzuki-Kamata, K. (1986) Characterisation of debris avalanche deposits in Japan, *Jo. Volcanol and Geothermal. Res*. **29,** 231-243.
318. Ulrhammer, R.A. (1996). Yosemite rock fall of July 10, 1996, *Seism. Res. Lett.* **67,** 47-48.
319. Vallance, J.W. and Scott, K.M. (1997) The Osceola mudflow from Mount Rainier: sedimentology and hazard implications of a huge clay-rich debris flow, *GSA Bulletin*, **109,** 143-163.
320. Vallance, J.W., Siebert, L., Rose Jr., W.I., Girón, J.R., and Banks, N.G., (1995) Edifice collapse and related hazards in Guatemala, *Jo. of Volc. and Geoth. Res*. **66**, 337 – 355.
321. van Bemmelen, R.W. (1970) *The geology of Indonesia. General geology of Indonesia and adjacent archipelago*, 2nd. Edition, vol. 1A, Matinhus Nijhiff, The Hague.
322. van Wyk de Vries, B., and Francis, P.W. (1997) Catastrophic collapse at stratovolcanoes induced by gradual volcano spreading, *Nature* **387**, 387-390.

323. van Wyk de Vries, B., Self, S., Francis, P.W., and Keszthelyi, L. (2001) A gravitational spreading origin for the Socompa debris avalanche, *Jo. Volc. Geotherm. Res*. **105**, 225-247.
324. Varnes, D.J., Radbruch-Hall, D.H., and Savage, W.Z. (1989) Topographic and structural conditions in areas of gravitational spreading of ridges in the western United States, *United States Geol. Surv. Prof. Paper* 1496, 28 p.
325. Voight, B. (Editor) (1978) *Rockslides and Avalanches 1: natural phenomena*. Elsevier, Amsterdam, 833 pp.
326. Voight, B. (Editor) (1979) *Rockslides and Avalanches 2 : engineering sites.* Elsevier, Amsterdam, 850 pp.
327. Voight, B. (2002) Structural stability of andesite volcanoes and lava domes, *Phil. Trans. R. Soc. Lond. Ser. A* **258**, 1663-1703.
328. Voight, B. and Elsworth, D. (1997) Failure of volcano slopes, *Géotechnique* **47**, 1-31.
329. Voight, B. and Sousa, J. (1994) Lesson from Ontake-san: a comparitive analysis of debris avalanche dynamics. *Eng. Geol.* **38**, 261-297.
330. Voight, B., Janda, R.J., Glicken, H., and Douglass, P.M. (1983) Nature and mechanics of the Mount St. Helens rockslide-avalanche of 18 May, 1980, *Géotechnique* **33**, 243-273.
331. Wadge, G., Francis, P.W., and Ramirez, C.F. (1995) The Socompa collapse and avalanche event, *Jo. Volc. Geoth. Res.* **66**, 309-336.
332. Waltham, T. (1996) Very large landslides in the Himalayas, *Geology Today* **12**, 181-185.
333. Wang, W-N., Chigira, M., and Furuya, T. (2003). Geological and geomorphological precursors of the Chiu-fen-erh-shan landslide triggered by the Chi-Chi earthquake in central Taiwan, *Eng. Geol*. **69**, 1-13
334. Ward, S.N. and Day, S. (2003) Ritter Island Volcano-lateral collapse and the tsunami of 1888, *Geophys. J. Int*. **154**, 891-902.
335. Watson. R.A. and Wright, H.E. (1969) The Saidmarreh Landslide, Iran, In S.A. Schumm and W.C. Bradley (eds.) *United States Contributions to Quaternary Research*, Geol. Soc. Am. Special Paper 123, p. 115-139.
336. Watters, R.J. (1983) A landslide induced waterflood-debris flow, *Bull. Int. Ass. Eng. Geol*. **28,** 177-182.
337. Wayne, W.J. (1999) The Allemania rockfall dam: a record of a mid-holocene earthquake and catastrophic flood in northwestern Argentina, *Geomorphology,* **27,** 295-306.
338. Waythomas, C.F. and Wallace, K.L. (2002) Flank collapse at Mount Wrangell, Alaska, recorded by volcanic mass-flow deposits in the Copper River lowland, *Can. Jo. Earth Sci*., **39**, 1257-1279.
339. Waythomas, C.F., Miller, T.P., and Beget, J.E. (2000) Record of Late Holocene debris avalanches and lahars at Iliamna Volcano, Alaska, *Jo. Volc. Geoth. Res.* **104**, 97-130.
340. Weidinger, J. T. (1998) Case history and hazard analysis of two lake-damming landslides in the Himalayas, *Jo. of Asian Earth Sci*.**16,** 323-331.
341. Weidinger, J.T., Wang, J. and Ma, N. (2002) The earthquake-triggered rock avalanche of Cui Hua, Qin Ling Mountains, P.R. of China – the benefits of a lake damming prehistoric natural disaster. *Quat. Internat*. **93-94**, 207-214.
342. Whitehouse, I.E. (1983) Distribution of large rock avalanche deposits in the central Southern Alps, New Zealand, *New Zealand Jo. Geol. Geophys*., **26**, 271-279.
343. Whitehouse, I.E. and Griffiths, G.A. (1983) Frequency and hazard of large rock avalanches in the central Southern Alps, New Zealand, *Geology* **11**, 331-334.
344. Wieczorek, G.F. (2002) Catastrophic rockfalls and rockslides in the Sierra Nevada, USA, In S.G. Evans and J.V. DeGraff (eds.), *Catastrophic landslides: effects, occurrence, and mechanisms*, Geol. Soc. Am. *Rev. Eng. Geol*., v. XV, pp. 165-190.
345. Wieczorek, G.F., Jakob, M., Motyka, R.J., Zirnheld, S.L., and Craw, P. (2003) Preliminary landslide-induced wave hazard assessment: Tidal Inlet, Glacier Bay National Park, Alaska, *United States Geol. Surv. Open-File Report* 03-100
346. Wieczorek, G.F., Snyder, J.B., Waitt, R.B., Morrisey, M.M., Uhrhammer, R.A., Harp, E.L., Norris, R.D., Bursik, M.I., and Finewood, L.G. (2000) Unusual July 10, 1996, rock fall at Happy Isles, Yosemite National Park, California, *GSA Bulletin* **112**, 75-85.
347. Wiles, G.C. and Calkin, P.E. (1992) Reconstruction of a debris-slide-initiated flood in the southern Kenai Mountains, Alaska, *Geomorphology*. **5**, 535-546.
348. Wise, D.U. (1963) Keystone faulting and gravity sliding driven by basement uplift of Owl Creek Mountains, Wyoming. *Bull. Am. Assoc. of Petrol. Geol.* **47**, 586-598.

349. Yarnold, J.C. and Lombard, J.P. (1989) A facies model for large rock-avalanche deposits formed in dry climates, In Colburn, I.P., Abbott, P.L., and Minch, J. (eds.) *Conglomerates in Basin Analysis: A Symposium Dedicated to A.G. Woodford*. Pacific Section S.E.P.M. v. 62, p. 9-31.

350. Zhou, C.H., Yue, Z.Q., Lee, C.F., Zhu, B.Q., and Wang, Z.H. (2001) Satellite image analysis of a huge landslide at Yi Gong, Tibet, China, *Quat. Jo. Eng. Geol*. **34**, 325-332.

351. Zolotarev, G.S., Fedorenko, V.S., and Vinnichenko, S.M. (1986) Ancient seismogenic and recent slides and slumps in Tajikistan (Central Asia), *Geol. Applic. e Idrogeol*., **21**, 149-157.